Annex 4

Kinetics of drop breakup during emulsification in turbulent flow

Nina Vankova,[1] Slavka Tcholakova,[1] Nikolai D. Denkov,[1*] Ivan. B. Ivanov[1] and Thomas Danner[2]

[1]*Laboratory of Chemical Physics & Engineering,*
Faculty of Chemistry, Sofia University, 1164 Sofia, Bulgaria

[2]*BASF Aktiengesellschaft*
GCT/P, L549, Ludwigshafen, Germany

*Correspondence:
Assoc. Prof. Nikolai Denkov
Laboratory of Chemical Physics & Engineering
Faculty of Chemistry, Sofia University
1 James Bourchier Ave., 1164 Sofia
Bulgaria
Phone: (+359-2) 962 5310
Fax: (+359-2) 962 5643
E-mail: ND@LCPE.UNI-SOFIA.BG

Key words: emulsification, turbulence, drop breakup, drop deformation, kinetics of emulsification.

ABSTRACT

Systematic set of emulsification experiments is performed to elucidate the role of several factors, which control the process of oil drop breakage during emulsification in turbulent flow. The experiments are performed at high surfactant concentration and low oil volume fraction to eliminate the contribution of drop-drop coalescence. As starting oil-water premixes we use emulsions containing monodisperse oil drops, which are generated by the method of membrane emulsification. By passing these premixes through a narrow-gap homogenizer, working in turbulent regime, we study the evolution of the number concentration of drops with given diameter, as a function of emulsification time. The experimental data are analyzed by using an original kinetic scheme, which takes into account the generation of drops of a given size (as a result of breakup of larger drops) and their disappearance (as a result of their own breakup process). The performed analysis allowed us to determine the rate constant of the process of drop breakup, as a function of drop diameter, hydrodynamic conditions during emulsification, and viscosity of the drop phase. The breakup rate constants, determined in this way, are compared with available theoretical expressions in the literature and their modifications. The comparison shows that the breakup rate constant can be considered as a product of: (a) frequency of collisions between drops and turbulent eddies, and (b) efficiency of drop breakup, which is related to the energy required for drop deformation and subdivision into smaller drops. The energy for drop deformation contains two contributions, originating from the drop surface extension and from the viscous dissipation inside the drop, respectively.

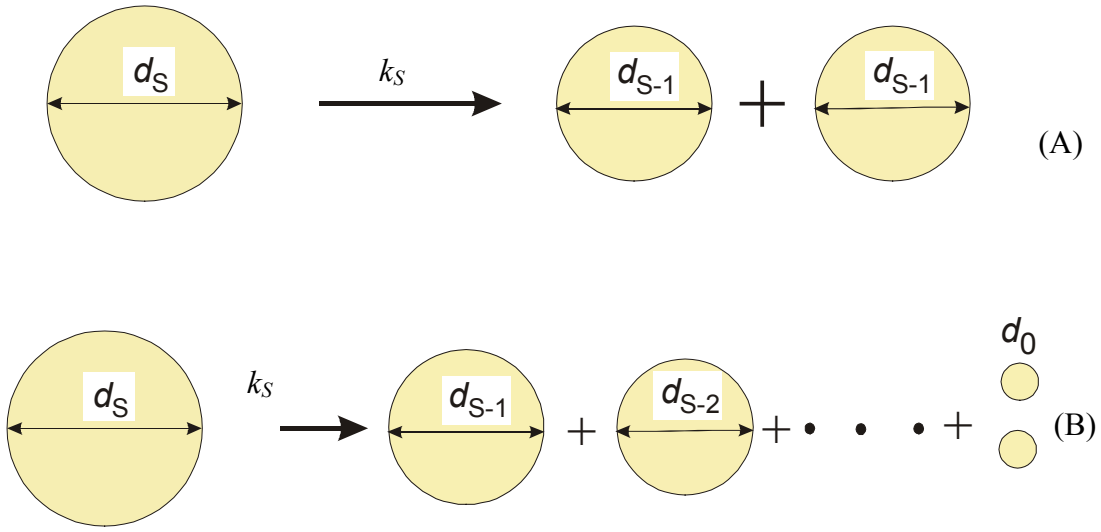

Schematic presentation of the processes of drop breakage.

1. Introduction.

The process of emulsification can be considered as consisting of two "elementary reactions": drop breakup leading to formation of several smaller drops from a larger one, and drop-drop coalescence leading to formation of larger drop from two smaller drops. The evolution of the drop-size distribution, during emulsification, depends on the competition between these elementary processes [1-6].

For quantitative analysis of these processes it is convenient to study them separately. Several studies were performed to clarify the main factors governing the steady-state drop size distribution in O/W emulsions, with very low oil volume fraction (lean emulsions), in which the contribution of drop-drop coalescence is negligible [7-13]. The classical studies of emulsification in turbulent flow by Kolmogorov [14] and Hinze [15] showed that the maximal diameter of stable drops is determined by the balance between the fluctuations in the hydrodynamic pressure of the continuous phase (which act on drop surface and thus lead to drop deformation), and the drop capillary pressure, which opposes drop deformation. A simple theoretical expression was derived in these studies, which relates the maximum diameter of stable drops with the rate of energy dissipation, ε, which is the main characteristic of the turbulent flow, and with the interfacial tension of the drops, σ_{OW} [14-15]. This expression was verified experimentally by Sprow [7], under various hydrodynamic conditions, for oil drops with viscosity close to that of the continuous aqueous phase.

Further development of the theory for more viscous drops, and the respective experimental verification for emulsification in stirred tanks, was presented by Lagisetty et al. [11] and Calabrese et al. [8-10]. Lagisetty et al. [11] suggested and tested a theoretical model for the maximum diameter of stable drops in turbulent flow, by including the possible effects of the non-Newtonian rheological behavior of the drop phase and of the time required for drop deformation and breakage. Similarly to Kolmogorov [14] and Hinze [15], Lagisetty et al. [11] used a stress balance to derive its expression for the maximum drop diameter. Calabrese et al. [8-10] used another approach, in which the energy required for drop deformation (for Newtonian drops) was compared to the kinetic energy of the turbulent eddies. Large set of experimental results for the effects of drop viscosity and interfacial tension on the maximum drop diameter is presented in the papers by Calabrese et al. [8-10], and a good agreement with the theoretical expressions was observed. For the hydrodynamic conditions in stirred tanks, like those used in refs 8-10, the interfacial tension was found to be the main factor, determining the mean drop diameter, for oils with viscosity between 1 and 100 mPa.s, whereas the oil viscosity was the predominant factor for more viscous oils.

Along with the steady-state drop size, the rate of drop breakage is another characteristic of the emulsification process, which is of great interest from both fundamental and practical viewpoints. Two main types of theoretical models for the rate of drop breakage in turbulent flow were considered in the literature. In the first type, the rate constant of drop breakage is constructed as a product of the characteristic frequency of drop deformation

(assumed equal to the reciprocal time of drop deformation) and the efficiency of drop breakage [1]. In the other type of models, the rate constant of drop breakage is considered as a product of the eddy-drop collision frequency and the efficiency of drop breakage [3-4]. In both cases, the efficiency of drop breakage is expressed as an exponent, including the ratio of the surface energy for drop deformation and the kinetic energy of the turbulent eddies, by analogy with the activation energy and the molecular kinetic energy in chemical kinetics. For determination of the eddy-drop collision frequency, Prince and Blanch [4] assumed that the drops and eddies of the same size behave as molecules in the kinetic theory of gases, and their mean velocities were calculated and used to find the collision frequency. Further development of this model was suggested in the same study by Prince and Blanch [4], and in a more recent study by Tsouris and Tavlaridies [2], who assumed that the drops could break even after collision with eddies having smaller size than the drops. Recently, Narsimhan [16] modified this model by describing the transport of drops and eddies through their turbulent diffusion coefficients. Further explanations about some of these models are given in section 6 below.

The models of the "elementary" process of drop breakage, described in the previous paragraph, were implemented in the so-called "population balance equation" for the temporal evolution of the drop-size distribution [1-4]. The population balance equation was tested with emulsification experiments, in the absence of surfactants, in which both drop breakage and coalescence were simultaneously present. Thus the verification of the drop breakage models was indirect, by using experimental data for the evolution of the mean drop diameter during emulsification in stirred tanks. Since the process of drop coalescence is still poorly understood [16], the used equations in the population balance model included expressions for the rate of drop-drop coalescence, which contained several adjustable parameters. Therefore, it was impossible to perform a direct, unambiguous verification of the drop breakage models in these studies, due to the interference between drop breakage and drop coalescence.

To the best of our knowledge, the only experimental data for the rate of drop breakage in the absence of coalescence, is presented by Narsimhan et al. [12-13]. In these studies [12-13], the change of drop-size distribution in the course of emulsification in stirred tanks was used to determine the breakage rate constant, as a function of drop volume. To interpret the experimental data, the so-called "similarity assumption" was used, which relates the probability for formation of daughter drops of given size with the dependence of the rate constants on drop volume (see refs 12-13 for further explanation). The experiments in refs 12, 13 were performed with oils having viscosity close to that of the continuous phase, so that the effect of oil viscosity on the kinetics of drop breakage was not studied.

In the current paper we describe emulsification experiments with oil-in-water emulsions aimed to further elucidate the role of several factors in the process of drop breakup in turbulent flow. The experiments are performed at relatively low oil volume fraction and high surfactant concentration to avoid the effect of drop coalescence. The studied emulsions are prepared with three relatively viscous oils – two silicone oils with viscosities 50 and 100 mPa.s, respectively, and soybean oil with viscosity 50 mPa.s. As starting oil-water premixes

we use emulsions containing monodisperse oil drops, which are generated by the method of membrane emulsification. By passing these premixes through a narrow-gap homogenizer, we determine the evolution of the drop-size distribution, as a function of emulsification time. The experimental data are analyzed by using a new kinetic scheme, which allows us to evaluate the dependence of the breakage rate constant on drop diameter. The possibility for formation of several "daughter" drops with various sizes is taken into account. The obtained values of the drop breakage constants are compared to theoretical models and, on this basis, some conclusions about the mechanism of drop breakage are drawn.

2. Materials and methods.

2.1. Materials. We used nonionic low molecular-mass surfactant polyoxyethylene-20 hexadecyl ether (Brij 58, product of Sigma), with concentration of 1 wt %, which is well above the critical micelle concentration of this surfactant (CMC $\approx 10^{-5}$ M $\approx$ 0.001 wt %). The concentration of NaCl was 150 mM. The aqueous solutions were prepared with deionized water from a Milli-Q Organex system (Millipore).

As dispersed phase we used several oils: soybean oil (SBO, commercial product) with viscosity of 50 mPa.s; silicone oil SH200C with viscosity 50 mPa.s (product of TDCS); and silicone oil Silikonöl AK100 (product of BASF) with viscosity 96 mPa.s. SBO was purified by passing it through a glass column, filled with Florisil adsorbent. The silicone oils were used as received.

2.2. Methods for emulsion preparation.

All emulsions, described in this chapter, were obtained in a two-step procedure, which includes two different experimental techniques: membrane emulsification to prepare an oil-water premix, and emulsification in turbulent flow by using a narrow-gap homogenizer. The exact emulsification protocol is described in section 2.3. In the following two subsections we present a brief description of the used emulsification methods.

2.2.1. Membrane emulsification.

This technique was applied to prepare initial emulsions (oil-water premixes) with relatively narrow drop size distribution. The method is based on the use of microporous membranes with pores of uniform size [17-18]. The membrane separates two immiscible liquids – dispersed phase (SBO, hexadecane or silicone oil in our experiments) and continuous phase (1 wt % Brij 58 + 150 mM NaCl). Dispersed phase is emulsified, by passing it through the membrane pores under pressure, into the continuous phase. In our experiments, we used a laboratory Microkit membrane emulsification module from Shirasu porous glass (SPG) Technology (Miyazaki, Japan) [19-21], which works with tubular glass membranes (of outer diameter 10 mm, thickness 1 mm, and working area of approximately 3 cm^2). Two

membranes, with mean pore size of 3.2 μm (denoted as SPG3.2 in the text) and 10.7 μm (denoted as SPG10.7), were used for preparing emulsions with two different drop size distributions. The working pressure difference across the membranes was 2.9×10^4 Pa for SPG3.2, whereas for SPG10.7 it was varied between 0.98 and 3.92 kPa, depending on oil viscosity.

2.2.2. Narrow-gap homogenizer. A custom-made modification of the narrow-gap homogenizer was used for the second stage of the emulsification process. A detailed description of this homogenizer is given in Chapter 3 of the Report - here we describe briefly only its most important components.

The apparatus consists of pipes, a turn-cock, and a cylindrical mixing chamber, equipped with a processing element, which has narrow slits inside the chamber. The slits in the processing element ensure high density of power dissipation, which leads to drop deformation and breakage inside the mixing chamber. For the experiments, discussed in this chapter, we used the processing element GW395-2C, which has two consecutive slits with gap-width of 395 μm. The volume, in which the turbulent dissipation of energy takes place, V_{DISS}, is estimated to be 1.72×10^{-7} m^3 for this processing element [22-23]. The construction of GW395-2C is described in Chapter 3 and is schematically shown in Figure 3.1A.

In the used equipment, the oil-water mixture is forced to pass through the emulsification element by applying a certain pressure at the inlet of the homogenizer. The driving pressure is provided by a gas N_2-bottle, connected by a Tygon hose to the fitting element between the vessel and the ingoing pipe for the emulsion, on one side, and the turn-cock, on the other side (see Figure 3.2 in Chapter 3). A pressure transducer is installed close to the gas bottle outlet, which enables precise regulation of the applied pressure during the emulsification (the pressure is maintained with an accuracy of ± 500 Pa in a given experiment). In several series of experiments the driving pressure was 1×10^5 Pa ± 800 Pa, whereas in other experimental series the pressure was higher, 2.2×10^5 Pa, to study the effect of hydrodynamic conditions on breakage rate constant. The construction of the used homogenizer enables emulsification in a discontinuous mode only - after each pass of the oil-water mixture through the homogenization element, the pressure is released and the emulsion is manually poured back into the inlet of the device for the next pass. The operating conditions, during emulsification of the systems studied, are given in Table 1. The oil viscosity and the interfacial tension, shown in Table 1, are measured by methods described in sections 2.5 and 2.6.

Table 1. Operating conditions during emulsification with processing element GW395-2C and $V_{DISS} = 1.72\times10^{-7}$ m^3. The continuous phase is 1 wt % Brij 58 + 150 mM NaCl ($\rho_c = 1.0044$ g/cm^3). The mean volume-surface diameter of the initial premix, prepared by membrane emulsification, d_{32}^{INI}; type of oil phase; oil volume fraction, Φ; viscosity of the oil phase, η_D; interfacial tension, σ_{OW}; applied pressure, p; flow rate, Q; calculated value of the density of power dissipation, ε; and the residence time, $\theta = V_{DISS}/Q$; are presented.

d_{32}^{INI}, μm	Oil phase	Φ	η_D, mPa.s	σ_{OW}, mN/m	Hydrodynamic conditions			
					$p\times10^5$, Pa	$Q\times10^{-3}$, m^3/s	$\varepsilon\times10^5$, J/(kg.s)	θ, ms
32.6	SBO	0.01	50	7.5 ± 0.1	0.9807	0.086	0.49	2.0
34.0	SBO	0.01	50	7.4 ± 0.1	2.20	0.15	1.92	1.1
35.2	Silicone oil	0.006	50	10.5 ± 0.1	1.00	0.092	0.53	1.9
34.4	Silicone oil	0.003	96	10.3 ± 0.1	1.01	0.096	0.56	1.8
11.1	SBO	0.0024	50	7.4 ± 0.1	2.20	0.16	2.05	1.1

2.3 Procedure for emulsion preparation.

Six series of experiments were performed, following a two-stage protocol of emulsion preparation:

First, a monodisperse initial emulsion (premix) was prepared by membrane emulsification. About 10 mL of the used oil was passed through the membrane pores, under a certain pressure, into 990 mL of 1 wt % aqueous solution of Brij 58 (+ 150 mM NaCl). In the experiments with membrane SPG10.7 monodisperse emulsions with an initial diameter d_{32}^{INI} = 33.2 ± 2.0 μm were obtained (see Table 1). Monodisperse initial emulsions with mean drop diameter of 11.1 μm were prepared with membrane SPG3.2. The pressure difference across membrane SPG3.2 was maintained at 29 ± 1 kPa, whereas the pressure across membrane SPG10.7 was 4 ± 1 kPa. The initial monodisperse emulsion, prepared by membrane emulsification, was gently homogenized by hand-tumbling and samples for determination of drop size distribution were taken with a pipette. The drop size distribution was determined by optical microscopy, as described in section 2.4 below.

The second homogenization step was accomplished by multiple passes of the emulsion through the narrow-gap homogenizer (see subsection 2.2.2). In each experiment, 100 passes of the emulsion through the homogenizer were performed. After each of the first 10 passes, and then after each fifth pass, at least two emulsion samples were taken for determination of the drop size distribution. Thus we determined the drop size distribution as a function of the number of passes (viz. of the emulsification time).

2.4. Determination of drop size distribution.

Drop size distribution in the emulsions was determined by optical microscopy. The oil drops were observed and video-recorded in transmitted light by means of microscope Axioplan (Zeiss, Germany), equipped with objective Epiplan, ×50, and connected to a CCD camera (Sony) and VCR (Samsung SV-4000). The diameters of the oil drops were measured, one by one, from the recorded video-frames, by using custom-made image analysis software, operating with Targa+ graphic board (Truevision, USA).

The mean volume-surface diameter, d_{32}, was calculated from the measured drop diameters by using the relation:

$$d_{32} = \frac{\sum_i N_i d_i^3}{\sum_i N_i d_i^2} \tag{1}$$

where N_i is the number of drops with diameter d_i.

2.5. Measurements of oil viscosity.

The viscosity of SBO and of silicone oils was measured on a Brookfield Rheoset laboratory viscometer, model LV (Brookfield Engineering Laboratories, Inc.), controlled by computer. Spindle CP-52 (cone-plate geometry, cone angle = 3° and radius 1.2 cm, viscosity range 50-10^5 mPa.s) or spindle CP-40 (cone-plate geometry, cone angle = 0.8° and radius 2.4 cm, viscosity range 10-10^3 mPa.s) was used. These measurements were performed at room temperature, 25 ± 1 °C.

2.6. Measurement of interfacial tension.

The oil-water interfacial tension was measured by using a drop-shape-analysis on pendant drops from the surfactant solutions, immersed in a bulk oil phase. The measurements were performed at 27 ± 0.5 °C on a Drop Shape Analysis System DSA 10 (Krüss GmbH, Hamburg, Germany). The mass density of the aqueous solutions and of the used oils was measured on a density meter DMA48 (Paar Scientific, UK) at 27 ± 0.1 °C. The accuracy of mass density determination is ± 0.001 g/cm^3.

3. Experimental results for the mean drop size versus number of passes of the emulsion through the homogenizer.

In this section we present experimental results about the mean volume-surface diameter, d_{32}, as a function of the number of passes of the emulsion through the narrow-gap homogenizer, u, for the various systems studied. The kinetic scheme used for calculation of the breakage rate constant, k_{BR}, is described in the next section. Experimental data about the

drop size distribution versus the number of passes, along with the procedure for interpretation of these data, are presented in section 5. The theoretical models used to analyze the obtained dependence of k_{BR} on drop diameter are described in section 6.

3.1. Mean drop diameter, d_{32}, as a function of the viscosity of the dispersed phase, η_D.

To study the effect of η_D on the evolution of the drop size distribution during emulsification, we performed three series of experiments with different oils, SBO with η_D = 50 mPa.s and two silicone oils with viscosities of 50 and 96 mPa.s, respectively.

The emulsions were prepared at equivalent operating conditions, following the procedure described in section 2.3. The initial emulsions were produced with membrane SPG10.7 and the mean volume-surface drop diameter was $d_{32}^{INI} \approx 34$ μm, see Table 1. The second homogenization step is performed at a driving pressure $p \approx 1\times10^5$ Pa, which corresponds to density of power dissipation $\varepsilon \approx 0.53\times10^5$ J/(kg.s). The mean drop diameter, d_{32}, obtained after passing the emulsion 100 times through the narrow-gap homogenizer, is presented in Table 2 for each of the studied systems. The results show that the initial mean drop size decreases about 2.6 times for the more viscous silicone oil (η_D = 96 mPa.s) and about 3.4 times for the oils with η_D = 50 mPa.s.

To compare the experimentally obtained values of d_{32} with the theoretical predictions of the theory of turbulent emulsification, we calculated the so-called "Kolmogorov-Hinze diameter", d_K [14-15,22-23]:

$$d \approx \varepsilon^{-2/5}\sigma_{OW}^{3/5}\rho_C^{-3/5} \qquad (2)$$

Here $\rho_C = 1.0044\times10^3$ kg/m^3 is mass density of the continuous phase, ε is rate of energy dissipation defined per unit mass and σ_{OW} is interfacial tension. The calculated values of d_K are also presented in Table 2.

Table 2. Experimental values of the final mean volume-surface diameter, d_{32}, for oils with different viscosities. The aqueous phase contains 1 wt % Brij 58 and 150 mM NaCl. The emulsification is performed at $p \approx 1\times10^5$ Pa with a processing element GW395-2C. The values of d_K are calculated from eq 2.

Oil phase	η_D, mPa.s	σ_{OW}, mN/m	d_{32}^{INI}, μm	d_{32}, μm	d_K, μm
silicone oil	96	10.6 ± 0.3	≈ 34.0	12.97	12.8
silicone oil	50			10.8	13.6
SBO	50	7.49		9.4	11.2

The differences in the calculated values of d_K originate from the slightly different values of ε in the various experiments and from the different interfacial tensions, σ_{OW}, of the oils.

As seen from Table 2, the experimental values of the final mean drop diameter, d_{32}, are in a good agreement with the theoretically predicted values of d_K. The ratio d_{32}/d_K is about 0.8 for the systems with η_D = 50 mPa.s and about 1.0 for the emulsion with η_D = 96 mPa.s.

The experimental values of d_{32} are plotted in Figure 1 as a function of the number of passes, u. The respective values of d_K are also indicated in the figure by horizontal lines. As seen from the figure, d_{32} gradually decreases with the number of passes. One observes that the decrease of d_{32} occurs in a very similar manner for the emulsions prepared with oils of similar viscosity (SBO and silicone oil with 50 mPa.s). Most rapidly d_{32} diminishes during the first ten passes: from 33 μm down to 19 μm for the SBO-emulsion and from 35 μm down to 18 μm for the silicone oil. During the next thirty passes (from u = 10 to u = 40) a further reduction of the mean drop size from 19 μm down to 12.5 μm is observed for the SBO-emulsion. Afterwards, d_{32} remains almost constant until the seventieth pass, and finally, a very slow decrease from 12.7 μm down to 9.4 μm is observed during the last 30 passes. For the silicone oil emulsion, a gradual decrease of d_{32} from 18 μm after the 10th pass down to 11.7 μm after the 60th pass is observed, followed by a steady-state drop size distribution with $d_{32} \approx 11$ μm during the last 40 passes.

For the emulsion, prepared with silicone of higher viscosity, η_D = 96 mPa.s, the mean drop size decreases much slower during the first ten passes, from 34 μm down to 26 μm. Afterwards, d_{32} continues to diminish, reaching the value of 13 μm at the end of the emulsification, see Figure 1. Obviously, the drop breakage process is much slower for the more viscous oil.

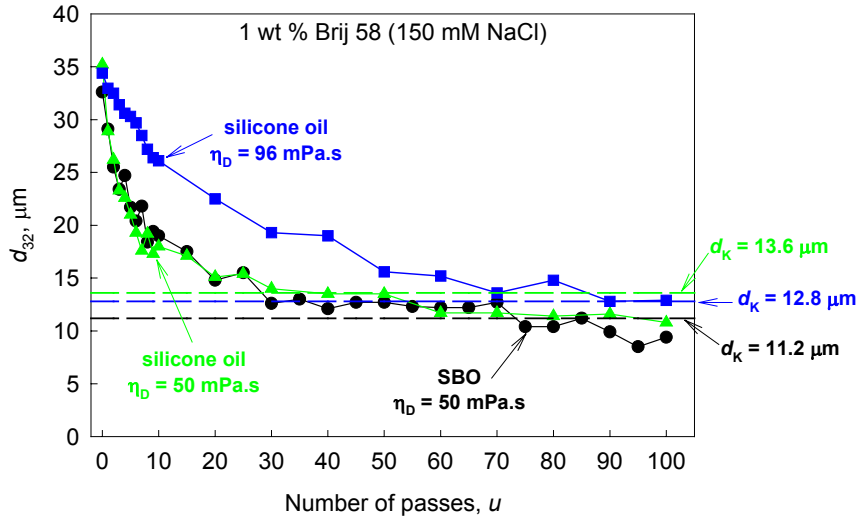

Figure 1. Experimentally obtained mean volume–surface diameter, d_{32}, as a function of the number of passes, u, and theoretically calculated d_K from eq 2 for 1 wt % Brij 58 -stabilized emulsions with different oil phases. The solutions contain 150 mM NaCl. Emulsification at $p \approx 1\times10^5$ Pa with a processing element GW395-2C.

3.2. Mean drop diameter, d_{32}, as a function of applied pressure.

In this section we present the experimental results for two SBO-in-water emulsions, prepared at two different driving pressures, $p = 0.98\times10^5$ Pa and $p = 2.2\times10^5$ Pa, ensuring flow rates of $Q = 0.086\times10^{-3}$ m^3/s and 0.15×10^{-3} m^3/s, respectively. These changes of the operating conditions lead to a significant difference in the magnitude of the average power density, ε, which is very important for the rate of drop breakage. The power dissipation rate can be estimated from the expression $\varepsilon = pQ/V_{DISS}$ [22-23]. For the emulsion, produced at the lower pressure ($p = 0.98\times10^5$ Pa), the value of ε is thus estimated to be almost 4 times lower than the one for $p = 2.2\times10^5$ Pa. The values of the final mean drop diameter, d_{32}, obtained after 100 passes are presented in Table 3, along with the respective magnitudes of p and ε, and the calculated values of d_K.

As expected, the obtained steady-state mean drop size, d_{32}, is smaller for the emulsion prepared at higher pressure (viz., at higher power density of energy dissipation). It is observed that after 100 passes through the homogenizer, the initial mean drop size $d_{32}^{INI} \approx 33$ μm decreases about 6 times at the higher ε, reaching the value of 5.4 μm, while d_{32}^{INI} decreases down to 9.4 μm (i.e. about 3.4 times) at the lower value of ε. As seen from Table 3, the experimentally obtained values of d_{32} agree relatively well with the predicted mean drop diameter, d_K - for both emulsions $d_{32}/d_K \approx 0.8$.

Table 3. Experimentally obtained values of the final mean volume-surface diameter, d_{32}, at different values of the power density, ε. The aqueous phase contains 1 wt % Brij 58 and 150 mM NaCl, the oil phase is SBO; $\sigma_{OW} \approx 7.4$ mN/m. The emulsification is performed at two different pressures with a processing element GW395-2C. The respective values of d_K, calculated from eq. 2, are also shown.

Hydrodynamic conditions		d_{32}^{INI}, μm	d_{32}, μm	d_K, μm
$p\times10^5$, Pa	$\varepsilon\times10^5$, J/(kg.s)			
0.9807	0.49	≈ 33.3	9.4	11.2
2.20	1.92		5.4	6.4

The experimental dependence of d_{32} on the number of passes, u, along with the calculated values of d_K, is presented in Figure 2. It is seen that for the emulsion, prepared at $p = 2.2\times10^5$ Pa (corresponding to $\varepsilon = 1.92\times10^5$ J/(kg.s)), even one pass through the processing element is sufficient to reduce the value of d_{32} by more than 2.5 times, from 34 down to 13.3 μm. During the next two passes, further decrease of d_{32} from 13.3 μm to 10.7 μm is observed, followed by a gradual decrease down to 7.5 μm between passes 3 and 15. Finally, a very slow decrease down to 5.4 μm is observed during the last 85 passes.

The dependence of d_{32} on the number of passes for the SBO-emulsion, produced at lower pressure (p = 0.98×10^5 Pa and ε = 0.49×10^5 J/(kg.s)), was described in section 3.1. Most importantly, no such rapid reduction of the mean drop size is observed after the first pass, at ε = 0.49×10^5 J/(kg.s) - d_{32} decreases only by 4 μm, from 33 down to 29 μm, after the first pass. These experimental observations imply that the value of ε is of great importance for the rate constant of drop breakage.

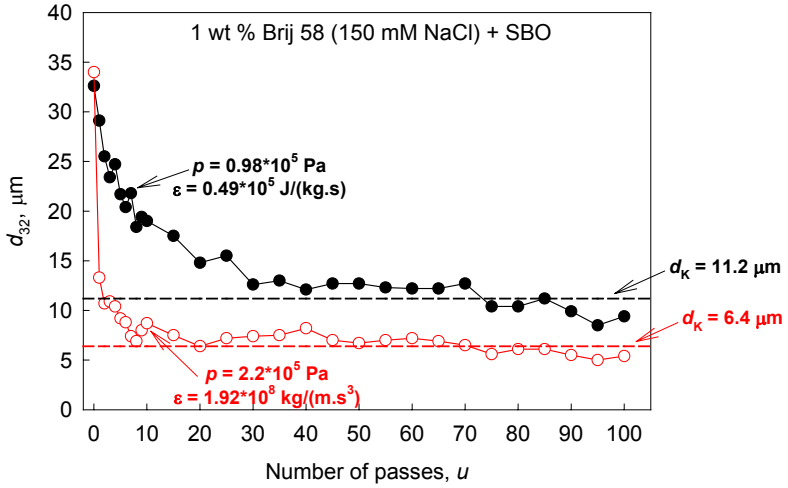

Figure 2. Experimentally obtained dependence of the mean volume-surface diameter, d_{32}, on the number of passes, u, and theoretically calculated d_K from eq. 2 for two SBO-in-water emulsions, prepared at different driving pressures. The aqueous phase contains 1 wt % Brij 58 and 150 mM NaCl. The emulsification is performed with a processing element GW395-2C.

3.3. Initial mean drop diameter, d_{32}^{INI}, as a factor affecting the rate of drop breakage.

In this section we describe experimental results, obtained with two SBO-in-water emulsions, which have different initial drop size distributions. One of the studied premixes was produced with membrane SPG10.7 and had an initial mean drop size of 34 μm. The other premix was prepared with membrane SPG3.2 and the respective mean drop size was 3 times smaller, d_{32}^{INI} = 11.1 μm. These initial emulsions were passed 100 times through the homogenizer at equivalent hydrodynamic conditions, p = 2.2×10^5 Pa and ε = 1.92×10^5 J/(kg.s) (processing element GW395-2C and V_{DISS} = 1.72×10^{-7} m^3). At the end of emulsification, after 100th pass, $d_{32}(u$=100) was 5.4 μm for the emulsion with d_{32}^{INI} = 34 μm, whereas $d_{32}(u$=100) was 7.8 μm for the emulsion with d_{32}^{INI} = 11.1 μm. The experimental values of d_{32}^{INI} and d_{32}, as well as the predicted drop diameter, d_K, are shown in Table 4. The theoretically estimated value, d_K, is one and the same for both emulsions, because the hydrodynamic conditions, the interfacial tension, and the mass density of the aqueous phase are identical in this series of experiments. However, as seen from the second column in Table 4, the final experimental values of d_{32} differ by about 30 % for these emulsions (despite the equivalent conditions during emulsification), which is beyond the experimental error. The latter result is somewhat surprising, but can be explained by comparing the volume-weighted histograms of the initial

emulsions (before the 1st pass, see Figures 3A and 3B), and of the final emulsions (after the 100th pass, Figures 3C and 3D). As one can see from Figure 3C, a relatively large fraction of very small drops, with size below Kolmogorov's diameter, d_K = 6.35 μm, is formed when the initial emulsion contains large drops. These small drops are called in the literature "satellite drops" [15] and they form in the breakage process of the large drops. The fraction of these satellite drops is much smaller in the other emulsion, which contains initially only drops with diameter comparable to Kolmogorov size (see Figures 3B and 3D). That is why, the final value of d_{32} for this emulsion is larger, although the initial mean drop size was smaller.

Besides, the results shown in Table 4 show that there is no unique constant of proportionality between the theoretically estimated d_K and the experimental, steady-state values of d_{32} – the ratio of these two diameters obviously depends on the initial drop size distribution, before starting the turbulent emulsification.

Table 4. Experimental values of the initial, d_{32}^{INI}, and final, $d_{32}(u=100)$ mean volume-surface diameters. The aqueous phase contains 1 wt % Brij 58 and 150 mM NaCl, the oil phase is SBO; $\sigma_{OW} \approx 7.4$ mN/m. The emulsification is performed at $p \approx 2.2\times10^5$ Pa ($\varepsilon = 1.92\times10^5$ J/kg.s) with a processing element GW395-2C. The respective value of d_K, calculated from eq 2, is also given.

d_{32}^{INI}, μm	d_{32}, μm	d_K, μm
34.0	5.4	6.35
11.1	7.8	

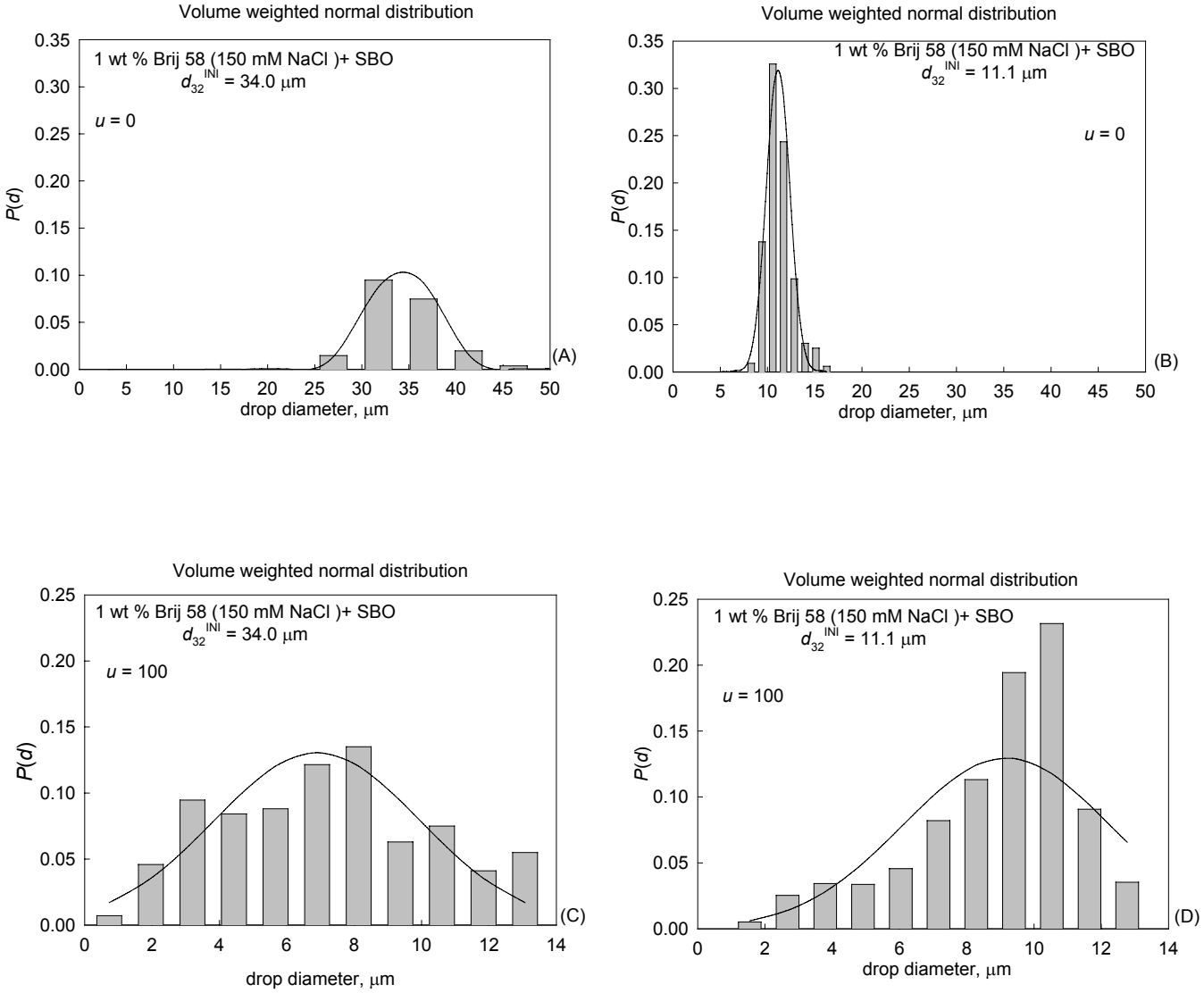

Figure 3. Initial (u = 0) and steady-state (u = 100) drop size distribution histograms, by volume, for two SBO-in-water emulsions with different initial drop diameters: (A) d_{32}^{INI} = 34 μm and (B) d_{32}^{INI} = 11.1 μm. The aqueous phase contains 1 wt % Brij 58 and 150 mM NaCl.

4. Kinetic scheme for the process of drop breakage.

In this section we present the model used for interpretation of the experimental data and for determination of the breakage rate constants. The main assumptions in the model are: (1) The drop-drop coalescence is negligible; (2) The drop breakage process is considered as an irreversible reaction of first order; (3) The drops in the emulsion are classified in a number of discrete intervals; all drops falling in a given interval are considered as having the same diameter, which corresponds to the average diameter in the interval; (4) The average drop diameter for a given interval is chosen in such a way, that the ratio of the drop volumes for two consecutive intervals is equal to two; (5) Differential equations are constructed for the evolution of the number concentration of the drops, falling in a given interval, under the assumption that the drop breakage occurs only in the processing element, which can be considered as a reactor of ideal displacement. The equations corresponding to these assumptions are specified in sections 4.1-4.3.

4.1. System under consideration

We consider a hypothetical system, which consists of drops having discrete set of volumes (diameters). The volume of the smallest drops in the system is denoted as v_0 and their diameter is d_0. The volumes of the larger drops in the system are $2v_0$, $4v_0$, $8v_0$, .., $2^N v_0$, respectively, where $2^N v_0$ is the volume of the largest drops in the emulsion. Therefore, the diameters of all drops in the system are d_0, $\sqrt[3]{2}d_0$, $\sqrt[3]{2^2}d_0$, …, $\sqrt[3]{2^N}d_0$. For simplification of the presentation we will denote the diameters as d_0, d_1, d_2,... d_N, where $d_S = \sqrt[3]{2^S}d_0$ and s is an integer number between 0 and N.

In the hypothetical system under consideration we have three qualitatively different types of drops. The largest drops in the system have a diameter d_N. These drops could break only and cannot be formed during emulsification (there are no larger drops to break and the drop-drop coalescence is suppressed). The drops having diameter larger than d_K (the Kolmogorov's diameter) and smaller than d_N can break and, simultaneously, can be formed as a product of breaking of larger drops. The third type of drops, which have a diameter smaller or equal to d_K could only be formed as a product of breakage of larger drops. The diameter of the drops dividing the third and second types of drop is assumed to be equal to the Kolmogorov's diameter, d_K, as estimated from eq 2. The comparison of the respective kinetic scheme with the experimental results (section 5) shows that these assumptions reflect the main experimental observations and allow us to (i) determine the rate constants of drop breakage, and (ii) gain information about the size distribution of daughter drops, obtained as a result of breakage of one larger drop.

4.2. Products of the drop breakage process

We assume that the breakage of drops having a diameter d_S ($k < s \le N$) leads to formation of several daughter drops with diameters d_0, d_1, ... d_{S-2}, and d_{S-1}, respectively. The fraction of the volume of the "mother" drop with diameter d_S, which is transformed into a drop with diameter d_m, where $0 \le m \le s-1$, is denoted as $p_{s,m}$. Hence, the value of $2^{s-m}p_{s,m}$ gives the average number of drops with diameter d_m, which are formed as a result of breakage of one drop with diameter d_S. The mass balance is satisfied, by imposing the condition that the drop with diameter d_S is transformed into smaller daughter drops, which have the same volume as the original drop. This mass balance can be expressed by the following equation:

$$\sum_{q=0}^{q-1} p_{S,q} = 1 \text{ for every } k < s \le N \tag{3}$$

where k is the index of the Kolmogorov's drops, which could not break and N is the number of the largest drops in the system.

4.3. Set of kinetic equations describing drop-size evolution

To formulate the kinetic equations, describing the drop size evolution, we assume that the drop breakage occurs only in the processing element, see Figure 4. The processing element is considered as a plug-flow reactor with ideal displacement, which is the simplest model for tubular-type of reactors [24]. This model implies that there is no longitudinal mixing of the fluid elements, as they move along the processing head of the homogenizer, and that all fluid elements travel for the same period of time from the inlet to the outlet of the equipment [24]. When the composition of the emulsion entering the processing element does not change with time (in a given pass), a steady-state drop-size distribution is established inside the reactor, and the function characterizing the evolution of drops with given size depends on the distance from the beginning of the reaction zone only [24], see Figure 4.

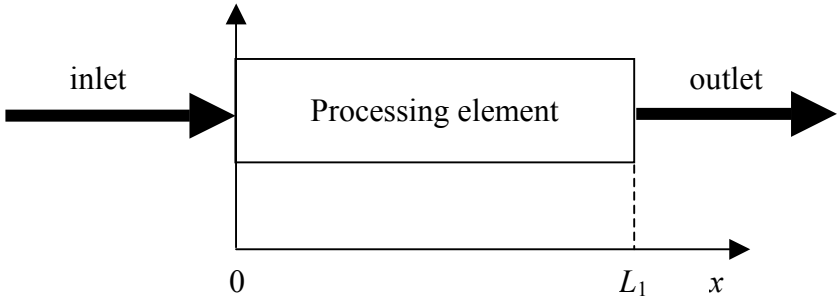

Figure 4. Schematic presentation of the processing element as a plug-flow reactor.

To formulate the differential equation desrcibing the evolution of the number concentration, n_S, of drops with size d_S, we assume that: the breakage process is an irreversible reaction of first order, a steady-state is reached immediately after starting the flow in a given pass, and $2^{s-m}p_{s,m}$ drops with size d_m are formed after breaking a drop with size d_S.

The differential equation describing the variation, along the processing element, of the concentration of the largest drops with diameter d_N is:

$$V_1 \frac{dn_N(x)}{dx} = -k_N n_N(x) \tag{4}$$

where V_1 is the linear velocity of the fluid along the processing element, x is the distance from the beginning of the element, k_N is the breakage rate constant and $n_N(x)$ is the concentration of the largest drops in the emulsion.

The differential equation, which describes the number concentration, n_S, of drops with diameter d_S, which could simultaneously break and form from larger drops during emulsification, is:

$$V_1 \frac{dn_S(x)}{dx} = -k_S n_S(x) + \sum_{q=S+1}^{N} 2^{q-S} p_{q,S} k_q n_q(x) \qquad for\ K < s \le N \tag{5}$$

where the first term in the right-hand side gives the rate of drop breakage, whereas the second term describes the rate of formation of these drops, as a result of breakage of larger drops. The parameter $2^{q-S}p_{q,S}$ gives the average number of drops with diameter d_S, which are formed from the breakage of drops with diameter d_q, where $q > s$.

As mentioned above, the drops with diameter smaller or equal to d_K could be formed only as a result of breakage of larger drops, which means that the first term in eq 5 is zero for these drops, and eq 5 is simplified to:

$$V_1 \frac{dn_S(x)}{dx} = \sum_{q=K+1}^{N} 2^{q-S} p_{q,S} k_q n_q(x) \qquad for\ 0 \le s \le K \tag{6}$$

where the index K indicates the Kolmogorov size.

The set of equations 4-6 was solved by using the initial conditions:

$$n_S(x=0) = n_S^0 \qquad for\ 0 \le s \le N \tag{7}$$

where n_S^0 is the number concentration of the drops with diameter d_S at the inlet of the equipment. Note that the values of n_S^0 are determined in our experiments by optical

microscopy - these are given by the drop-size distribution of the emulsion, poured into the inlet of the equipment for a given pass.

The solution of eqs 4-6 is:

$$n_N(x) = n_N^0 \exp\left(-\frac{k_N x}{V_1}\right) \tag{8}$$

$$n_S(x) = \exp\left(-\frac{k_S x}{V_1}\right)\left(const + \frac{1}{V_1}\sum_{q=S+1}^{N} 2^{q-S} p_{q,S} k_q \int \exp\left(\frac{k_S x}{V_1}\right) n_q(x)\,dx\right) \quad for\ K < s \le N-1 \tag{9}$$

$$n_S(x) = n_S^0 + \frac{1}{V_1}\sum_{q=K+1}^{N} 2^{q-S} p_{q,S} k_q \int_0^x n_q(\xi)\,d\xi \qquad for\ 0 \le s \le K \tag{10}$$

Note that the integrals for $n_S(x)$ in eqs 9 and 10 can be evaluated analytically, after the analytical expressions for the concentrations of the larger drops $n_q(x)$ are obtained by solving the respective equations for drops with size d_q ($q > s$).

Experimentally we measure the drop number concentration at the outlet of the equipment, see Figure 3.2. This concentration is given by eqs 8-10 with $x=L_1$. After substituting $x=L_1$ and taking into account that L_1/V_1 is the average residence time of the drops in the processing element, θ, we obtain expressions for the concentration of the drops with different sizes at the outlet of the equipment after the first pass through the homogenizer. For the largest drops the result reads:

$$n_N(x = L_1) = n_N^0 \exp\left(-\frac{k_N L_1}{V_1}\right) = n_N^0 \exp(-k_N \theta) \tag{11}$$

The solution for the number concentration of the second fraction of drops, n_{N-1}, with a diameter d_{N-1}, is:

$$n_{N-1}(x = L_1) = \left(n_{N-1}^0 - \frac{2 p_{N,N-1} k_N n_N^0}{k_{N-1} - k_N}\right)\exp(-k_{N-1}\theta) + \frac{2 p_{N,N-1} k_N n_N^0}{k_{N-1} - k_N}\exp(-k_N \theta) \tag{12}$$

where k_{N-1} and k_N are the breakage rate constants for drops having diameters d_{N-1} and d_N, respectively; n_{N-1}^0 and n_N^0 are their initial concentrations; $2p_{N,N-1}$ gives the average number of drops with diameter d_{N-1} which are formed after breakage of a drop with diameter d_N; and θ is the residence time of the drops in the processing element. It is clearly seen from eq 12 that the concentration of drops with diameter d_{N-1}, at the outlet of the processing element, depends not only of their rate of breakage, but also on the rate of their formation from the largest drops

(see the second term in the right-hand side of eq 12). In a similar way, one can derive expressions for the number concentrations of the smaller drops in the emulsion.

To describe the evolution of the number concentration of the various drops, after different number of passes through the homogenizer, we solve eqs 4-6 by using as initial conditions the concentrations, which are obtained as solutions of the same equations for the previous pass. For example, for the second pass through the homogenizer we solve eq 4 for the largest drops, by using eq 11 instead of eq 7 as an initial condition. In this way we are able to obtain analytical expressions for the number concentrations of the drops, as functions of the number of passes through the homogenizer, *u*. For the largest drops, the respective equation reads:

$$n_N(u) = n_N^0 \exp(-uk_N\theta) \tag{13}$$

where *u* is the number of passes of the emulsion through the homogenizer and n_N^0 is the number concentration of the drops in the initial premix, before the first pass. Note that $u\theta$ gives the total time of emulsion passage through the processing element, that is the total emulsification time.

The respective equation for the drops with diameter d_{N-1} is

$$n_{N-1}(u) = \left(n_{N-1}^0 - \frac{2p_{N,N-1}k_N n_N^0}{k_{N-1} - k_N} \right) \exp(-uk_{N-1}\theta) + \frac{2p_{N,N-1}k_N n_N^0}{k_{N-1} - k_N} \exp(-uk_N\theta) \tag{14}$$

In a similar way we derived equations, which describe the evolution of the number concentration of all drops in the emulsion. The equations for the smaller drops are rather long and will not be represented here.

4.4. Particular cases.

The constructed set consists of *N+1* equations, describing the evolution of the number concentration of drops with diameters between d_0 and d_N, plus *N-K* equations expressing the mass balance of the drops, which are able to break, see eq 3. On the other hand, we have *N-K* unknown breakage rate constants for the drops larger than d_K, as well as *(N-K)(N+K+1)/2* unknown constants of type $p_{s,m}$. Since the total number of unknown constants is larger than the total number of equations, we should make some assumptions for the constants $p_{s,m}$ to solve the set of equations. In this subsection we consider two simple illustrative cases. The comparison of these simple models with the experimental data shows that neither of them is able to describe adequately all our experimental results. That is why, another more complex model is considered in section 5.2C.

4.4.A. Binary breakage. The simplest case for drop breakage is the so-called "binary breakage" [12-13,25]. In our terms, this mode of drop breakage implies that only drops with equal diameters, d_{S-1}, are formed after breakage of a drop with diameter d_S ($K < s \leq N$). This process of drop breakage is schematically presented in Figure 5A. The assumed mode of drop breakage implies that $p_{S,S-1} = 1$ and all other values $p_{S,m} = 0$ for $m \leq s-2$. In this version of the model, we could easily determine the breakage rate constants from the experimental data for all drops with sizes larger than d_K. Note, however, that the formation of drops with diameter smaller than d_K is impossible in the binary breakage model. The latter restriction is in obvious contradiction with the experimental results, because a significant fraction of drops with diameter smaller than d_K was observed in the final emulsions, even when the premix did not contain any drops with such small diameters, see Figure 3.

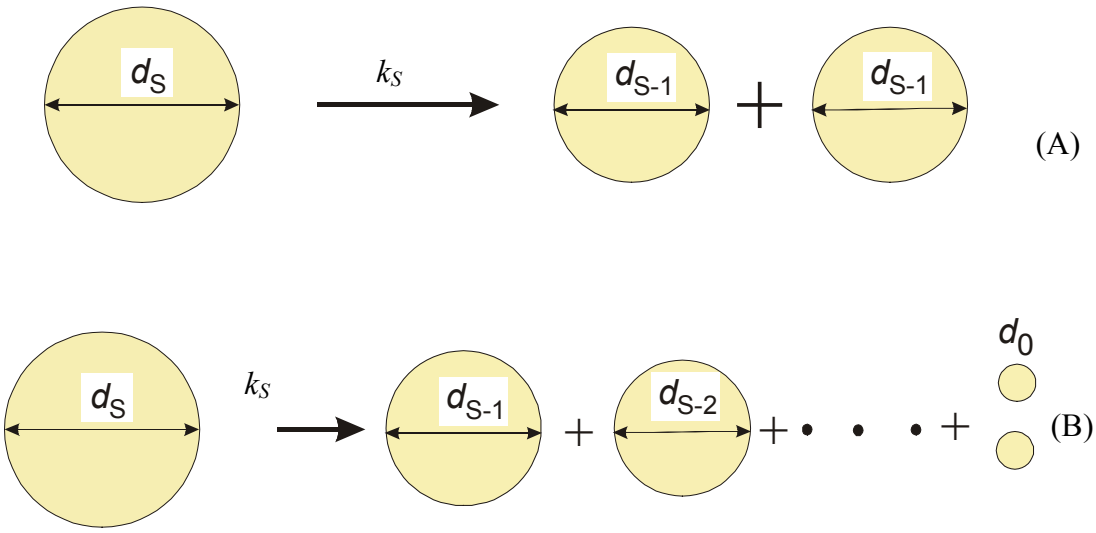

Figure 5. (A) Schematic presentation of the process of binary drop breakage. One drop with diameter d_S breaks into two smaller drops with equal diameters d_{S-1}, with a breakage rate constant, k_S. (B) Schematic presentation of the process of equal number probability breakage. One drop with diameter d_S breaks into a series of smaller drops with diameters d_{S-1}, d_{S-2}, .., d_1 (one drop for each size) and two drops with diameter d_0 (to satisfy the mass balance)

4.4.B. Equal number probability for drop formation. Another hypothetical case, which leads to relatively simple closed set of equations, can be designed if one assumes that the breakage of a drop with diameter d_S results in the formation of a series of single drops with diameters d_{S-1}, d_{S-2} ..d_1, plus two drops with diameter d_0 (to satisfy the mass balance for the breaking drop, eq 3), see Figure 5B. In this case, the probability for formation of smaller drops from a larger drop with diameter d_S is expressed by the equations:

$$p_{S,q} = \frac{1}{2^{S-q}} \qquad for\ 1 \le q \le s-1 \qquad \text{and}\ \ p_{S,0} = \frac{1}{2^{S-1}} \tag{15}$$

In the framework of this model, we should determine only the breakage rate constants from the experimental data, because the values of $p_{S,q}$ are pre-defined by eqs 15. Note that this model allows the formation of drops with diameter smaller than d_K. As shown in section 5.2, our experimental data are better described by this model (though not perfectly well), as compared to the model of binary breakage.

4.4.C. Numerical simulations. To check how the values of $p_{S,m}$ affect the dependence of the number concentration of drops with diameter d_m on the number of passes, $n_m(u)$, we performed numerical calculations of $n_m(u)$ for a hypothetical system, which consists of drops with 10 different diameters, ranging from d_0 to d_9. The drop diameter corresponding to d_K was chosen to coincide with d_5. In other words, drops with diameters between d_6 and d_9 could break into smaller drops, whereas the drops with diameter between d_0 and d_5 could only be formed as a result of breakage of larger drops. Additionally, we assume that only drops with diameter d_9 and concentration n_9^0 are present in the initial emulsion (i.e. the initial emulsion is monodisperse). For this illustrative simulation we take the following values of the breakage rate constants: k_9 = 100 s^{-1}; k_8 = 30 s^{-1}; k_7 = 10 s^{-1}; k_6 = 3 s^{-1} and θ = 1 ms. These values are close to the ones determined experimentally for some of the studied emulsions - see section 5 below.

From eq 13 one can see that the dependence $n_9(u)$ for the largest drops does not depend on the values of $p_{S,m}$, because the largest drops can only break. The situation for the smaller drops, which could both break and form from larger drops, is rather different. The comparison of the two theoretical curves, calculated from eq 14 for the two simplest cases described in sections 4.4A and 4.4B, is presented in Figure 6. It is seen that the maximal value of n_{N-1} changes around 2 times while changing $p_{N,N-1}$ from 1 (model of binary breakage) to 0.5 (equal number probability). Furthermore, the increase of n_{N-1} before the maximum in the curve is much steeper in the case of binary breakage, as compared to the case of equal number probability, see Figure 6.

The detailed mechanism of drop breakage and the distribution of daughter drops become even more important for the concentration evolution of the smaller drops. As an example, in Figure 7 we show theoretically calculated curves $n_K(u)$ for the drops having Kolmogorov's diameter (in our hypothetical example, $d_K = d_5 = d_{N-4}$).

In conclusion, the actual value of the probability for formation of smaller drops, as a result of breakage of the larger drops, affects significantly the dependence $n_m(u)$ for all drops with diameter smaller than d_N.

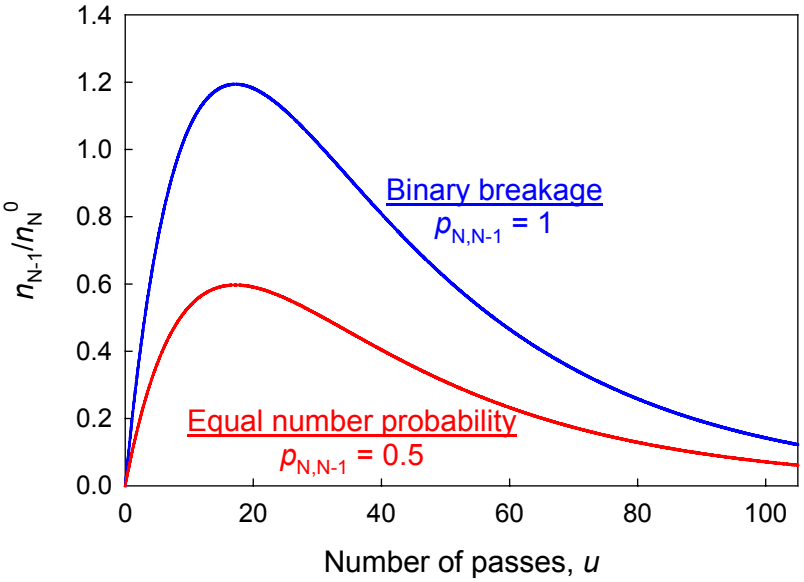

Figure 6. Normalised number concentration, n_{N-1}/n_N^0, of the second fraction of drops with diameter d_{N-1}, as a function of the number of passes, u, calculated by using eq 12 under the assumption of binary breakage (blue curve) or equal number probability for drop formation (red curve). The other parameters used in these calculations are k_N = 100 s^{-1}, k_{N-1} = 30 s^{-1}; θ = 1 ms and n^0_{N-1} = 0.

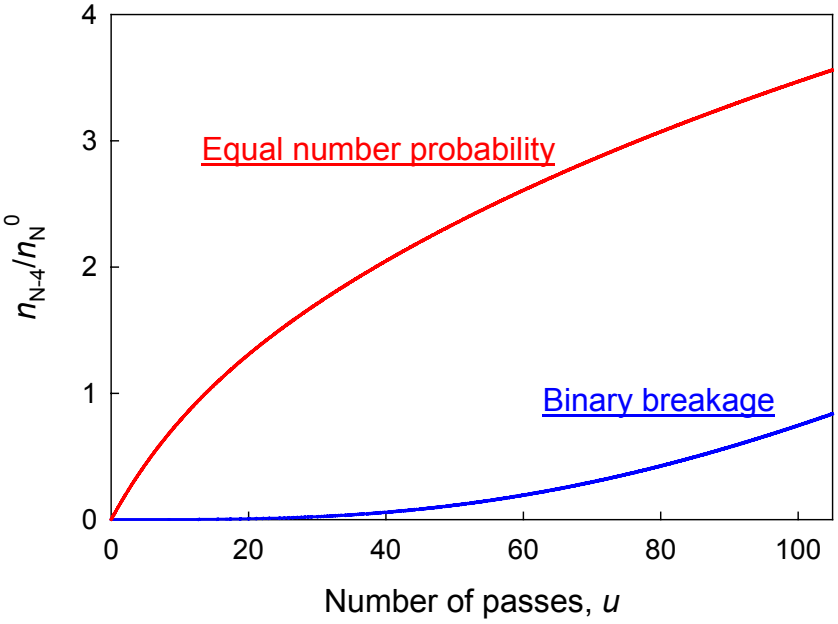

Figure 7. Normalised number concentration, n_{N-5}/n_N^0, for the drops with Kolmogorov's diameter, as a function of the number of passes, u, calculated under the assumption of binary breakage (blue curve) or equal number probability for drop formation (red curve). The other parameters used in these calculations are k_N = 100 s^{-1}, k_{N-1} = 30 s^{-1}; k_{N-2} = 10 s^{-1}; k_{N-3} = 3 s^{-1}; θ = 1 ms, and $n^0_{N-1} = n^0_{N-2} = n^0_{N-3} = n^0_{N-4} = 0$.

5. Interpretation of the experimental data and determination of the breakage rate constants

5.1. Data processing

For determination of the breakage rate constants we need to know how the number concentration of the drops with given size changes after passing the emulsion through the homogenizer. To obtain the dependence $n_S(u)$ we classified the experimental data for the drop size distribution inside discrete intervals. The average diameters in these intervals correspond to d_0, d_1, d_2,.d_S.. d_N, where $d_S = \sqrt[3]{2^S} d_0$ and d_0 is chosen in such a way that the Kolmogorov size corresponds to the average diameter of some of the intervals. The boundaries of the interval with average diameter d_i are d_i-x_i and $d_i + x_i$, whereas the boundaries of the interval with average diameter d_{i+1} are d_{i+1}-x_{i+1} and d_{i+1}+x_{i+1}, respectively ($x_i \neq x_{i+1}$). The ratio of the widths of the intervals around d_i and d_{i+1}, viz. the ratio x_i/x_{i+1}, was chosen to be equal to the ratio d_i/d_{i+1} [26]. The above requirements lead to the following boundaries of the intervals:

$$\left.\begin{aligned} & d_{i+1} - d_i = x_i + x_{i+1} \\ & \frac{2x_{i+1}}{2x_i} = \frac{d_{i+1}}{d_i} \\ & d_i = 2^{i/3} d_0 \end{aligned}\right\} \quad \Rightarrow \quad 0.885 d_i < d_i < 1.1150 d_i \quad (16)$$

Following the described procedure, we classified the measured drop diameters in different intervals and determined the number of drops falling in a given interval. To obtain the number concentration, n_S, of the drops falling in the interval around d_S, we used the following equation:

$$n_S = \frac{N_S}{V_{EM}} = \frac{N_S \Phi}{V_{OIL}} = \frac{6\Phi}{\pi} \frac{N_S}{\sum_{i=0}^{N} N_i d_i^3} \quad (17)$$

where N_i is the number of measured drops with diameter d_i, Φ is the oil volume fraction, V_{EM} is the emulsion volume, and V_{OIL} is the total volume of emulsified oil.

Typical histograms for the initial emulsion (premix), as well as for the same emulsion after 1, 20 and 100 passes through the homogenizer, are presented in Figure 8. It is seen that the number concentration of the smallest drops increases steeply after the first pass, whereas the number concentration of the largest drops decreases, due to their breakup. From such histograms we can construct the dependence $n_S(u)$, which is shown in Figure 9 below.

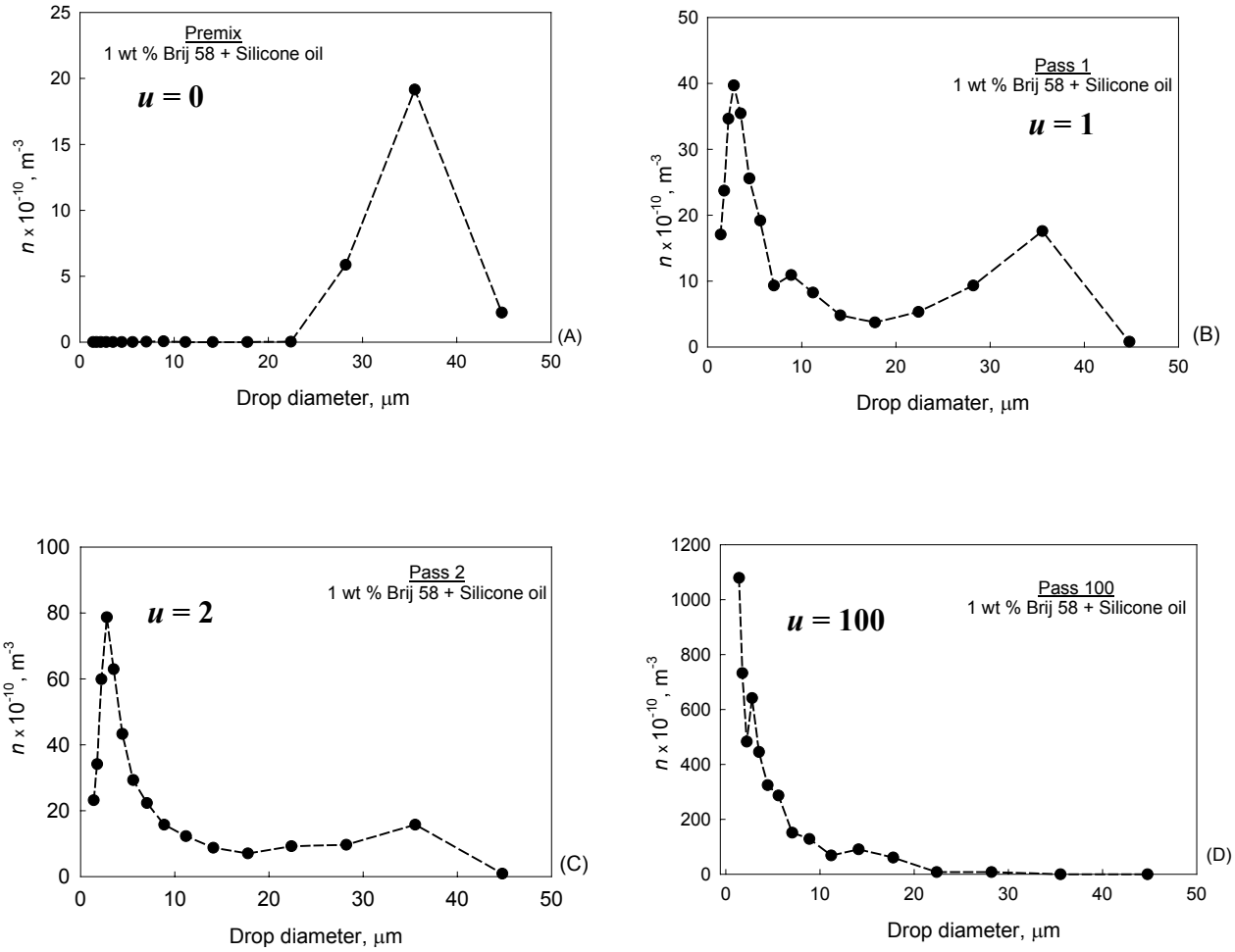

Figure 8. Number concentration of drops, as a function of drop diameter, for silicone oil-in-water emulsion, η_D = 50 mPa.s, stabilized by 1 wt % Brij 58 (+150 mM NaCl) for: (A) premix; (B) after 1 pass; (C) after 2 passes; (D) after 100 passes through the homogenizer.

5.2. Determination of breakage rate constants.

The kinetic scheme, described in section 4, shows that the evolution of the number concentration of the largest drops, n_N, does not depend on the breakage of the other drops, see eq 13. In other words we can determine k_N without knowing how the smaller drops break, whereas for determination of the breakage rate constant of the next fraction of drops, k_{N-1}, we need to know $p_{N,N-1}$ (viz. the probability for formation of drops with diameter d_{N-1} in the process of breakage of drops with diameter d_N). Note that the value of $p_{N,N-1}$ is not known in advance. The problem for determination of the rate constant for even smaller drops, k_{N-2}, is much more complex, because these drops could form in the process of breakage of the larger drops with diameters d_N and d_{N-1}. Thus, to describe the dependence of $n_{N-2}(u)$ we need the values of k_N, k_{N-1}, k_{N-2}, $p_{N,N-1}$, $p_{N,N-2}$, $p_{N-1,N-2}$.

To illustrate the procedure for determination of the breakage constants from the experimental data, we first demonstrate the data analysis by the two simple models, described

in section 4.4 above (models of binary breakage and equal number probability). In these models, the values of $p_{S,m}$ are fixed and from the best fit of the experimental data we can determine the values of the breakage rate constants. Note that the values for the drops larger than d_S (viz. k_{S+1}, k_{S+2}, .. k_N), which are determined from the best fits to the number concentrations of the respective drops (i.e. with diameters d_{S+1}, d_{S+2}, .. d_N) are introduced in the kinetic equation for n_S, so that the only adjustable parameter in this equation is k_S, which is used to fit the experimental data for $n_S(u)$.

5.2.A. Binary breakage. We were able to describe only the experimental data for $n_N(u)$ (largest drops in the premix) and for $n_{N-1}(u)$ (second fraction of drops) by this model. The experimental data for $n_N(u)$ and $n_{N-1}(u)$ for silicone oil-in-water emulsion, stabilized by 1 wt % Brij 58 (+150 mM NaCl), along with the best fit calculated by using eqs 13 and 14, are presented in Figures 9A and 9B, respectively. It is seen that the theoretical fits describe well the experimental data for these two fractions of drops. The values of k_N and k_{N-1} obtained from the best fits are 293 s^{-1} and 144 s^{-1}, respectively.

Note that the initial concentration of the largest drops, n_N^0, is around 10 times lower than n_{N-1}^0, see Figure 8A. For this reason, the contribution of the flux from the largest drops to n_{N-1} is relatively small, in comparison with the initial concentration of the drops with diameter d_{N-1}, see eq 14. The situation is different for the smaller drops with diameter d_{N-2}, see Figure 9C. Their initial concentration is around 3 times lower than n_{N-1}^0, and the contribution of the breaking larger drops, with diameters d_{N-1} and d_N, is very significant. Thus, from the dependence of n_{N-2} we could obtain information not only for the breakage constant of the drops with diameter d_{N-2}, but also for the breakage process of the larger drops. The numerical checks showed that it is impossible to describe the experimental data for $n_{N-2}(u)$ in the framework of the binary breakage model, see Figure 9C. One can see from this figure that the theoretical curve $n_{N-2}(u)$ increases much faster than the experimental points in the first 10 passes, which means that the binary breakage model grossly overestimates the flux from the larger drops to n_{N-2}.

Furthermore, we could determine the breakage rate constant for drops with diameter d_{N-2} by using only the passes, in which these drops have remained the largest ones in the emulsion. For this particular fraction of drops this happens after the 25th passes of the initial emulsion through the homogenizer, see Figures 9A and 9B. Note that the drops with diameters d_N and d_{N-1} disappeared completely from the emulsion after 25 passes, due to their faster breakage – hence, the drops with size d_{N-2} cannot be formed from larger drops, they can only break in the processing element. Thus we analyzed the experimental data for $n_{N-2}(u)$, starting from the 25th pass, by using eq 13 and obtained a breakage rate constant of k_{N-2} = 24 s^{-1}. Our attempt to fit the whole curve for $n_{N-2}(u)$ with this value of k_{N-2} were unsuccessful, see the blue curve in Figure 9 C. All experimental points fall below the theoretical curve, which means that the contribution of the drops, formed from breakage of larger drops, is

overestimated. In conclusion, the comparison between the experimental data and the theoretical curves clearly shows that the breakage of the largest drops in the studied emulsions does not occur through binary breakage, see Figure 9C.

If we try to describe the evolution of even smaller drops in the emulsion under consideration, the discrepancy between the theoretical predictions and the experimental data becomes more pronounced. Similar discrepancy between the experimental data and the theoretical predictions of the binary breakage model was established for all studied emulsions. Thus we can conclude that the binary breakage is not operative in any of the studied systems.

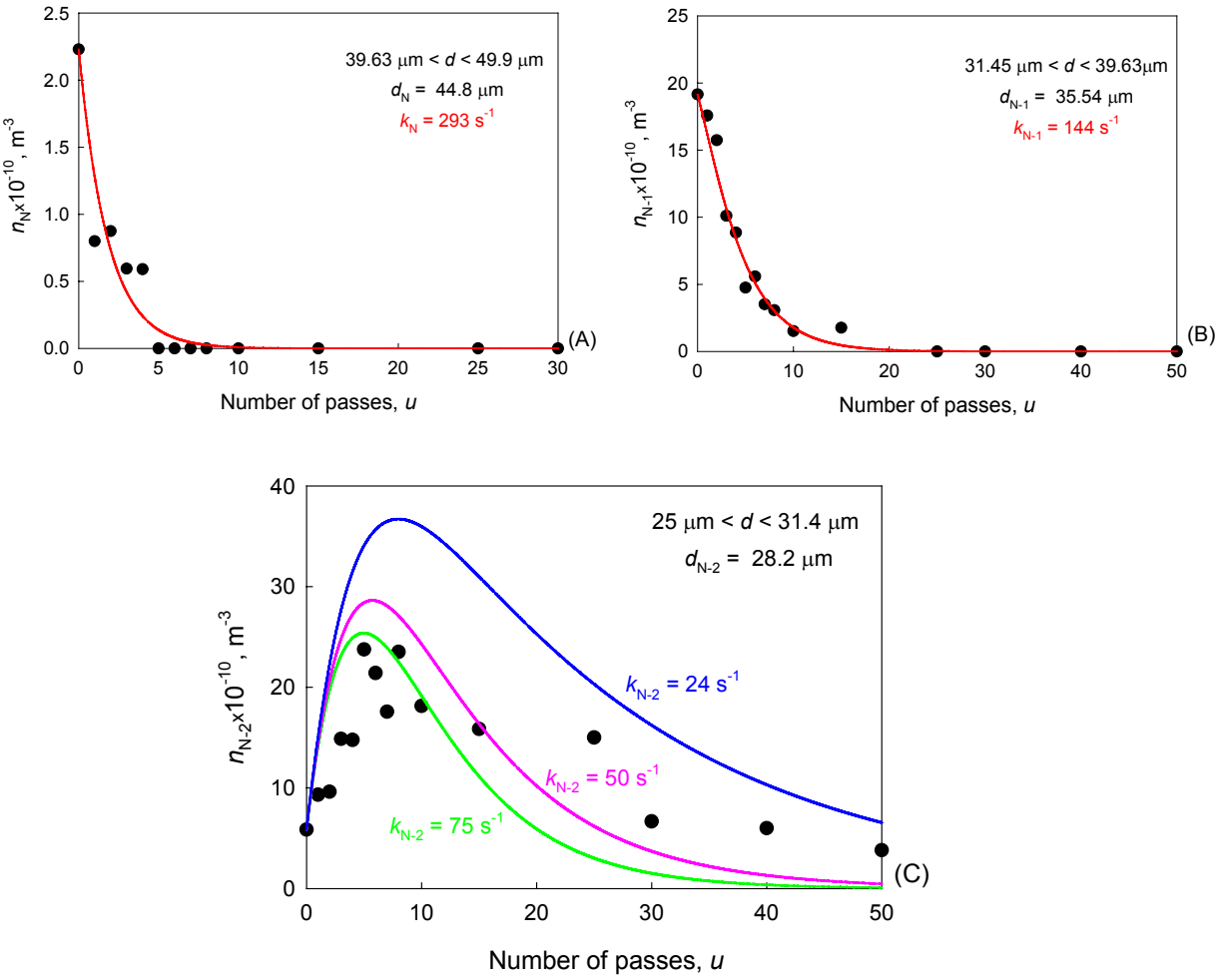

Figure 9. Number concentration of the drops, as a function of number of passes, along with the best fit constructed under the assumption for binary breakage for: (A) Largest drops in the initial emulsion having diameters between 39.6 and 49.9 μm; (B) Second fraction of drops with diameters between 31.5 and 39.6 μm; and (C) Third fraction of drops with diameters between 25 and 31.5 μm for silicone oil-in-water emulsions, stabilized by 1 wt % Brij 58 (+150 mM NaCl) at $\Phi = 0.01$.

5.2.B. Equal number probability for formation of smaller drops. In this subsection we present a comparison between the experimental results for $n_S(u)$, obtained with silicone oil-in-water emulsions with η_D = 50 mPa.s, and theoretical dependencies, calculated under the assumption that the values of $p_{S,m}$ are presented by eq 15. In this theoretical model, the breakage of a drop with size d_S leads to formation of a series of single drops with diameters d_{S-1}, d_{S-2}, ..., d_1, and two drops of diameter d_0, see Figure 5B. Thus we have explicit expressions for the dependence $n_S(u)$ with one unknown parameter, k_S. The values of k_{S+q} are known from the best fit to the data for the respective larger drops, $n_{S+q}(u)$.

The value of k_N for the largest drops in the emulsion for this particular emulsion is 293 s^{-1}, see Figure 9A. For the second fraction of drops with diameter d_{N-1} (between 31.5 and 39.6 μm) we obtain k_{N-1} = 128 s^{-1}, which is close to the value 144 s^{-1} obtained in the binary breakage model. The relatively low effect of $p_{N,N-1}$ on the fitted value of k_{N-1} is explained by the low initial concentration of the largest drops in the particular premix, which leads to a relatively low contribution of the largest drops in the function $n_{N-1}(u)$.

As explained in the previous subsection, we found that the evolution of the third fraction of drops with diameter d_{N-2} cannot be described under the assumption for binary breakage, see Figure 9C. On the other hand, the model of equal number probability, $p_{N,N-1}$ = $p_{N-1,N-2}$ = 0.5 and $p_{N,N-2}$ = 0.25, describes relatively well the experimental dependence $n_{N-2}(u)$. As seen from Figure 10A, the calculated curve follows the experimental data, and the value k_{N-2} = 24 s^{-1}, determined from the best fit of the whole curve, is in a good agreement with the constant obtained from the fit of the experimental data after the 25th pass only (when these drops are the largest ones in the emulsion).

Relatively good agreement between the experimental data and the theoretically calculated drop concentrations is observed for the drops with diameters d_{N-3} and d_{N-4}, as well (see Figures 10B and 10C). However, the comparison between the experimental data and the theoretical dependence $n_K(u)$ for the drops with the Kolmogorov size, equivalent to d_{N-5} in this system, shows that the flux from the larger drops to $n_K(u)$ is overestimated, see Figure 10D. On the other hand, the flux from the breaking large drops to the drops with diameter smaller than the Kolmogorov size is underestimated, see Figure 10E.

In conclusion, the model of equal number probability describes better the experimental data than the model of binary breakage, but it still cannot predict properly the formation of small drops with $d \le d_K$.

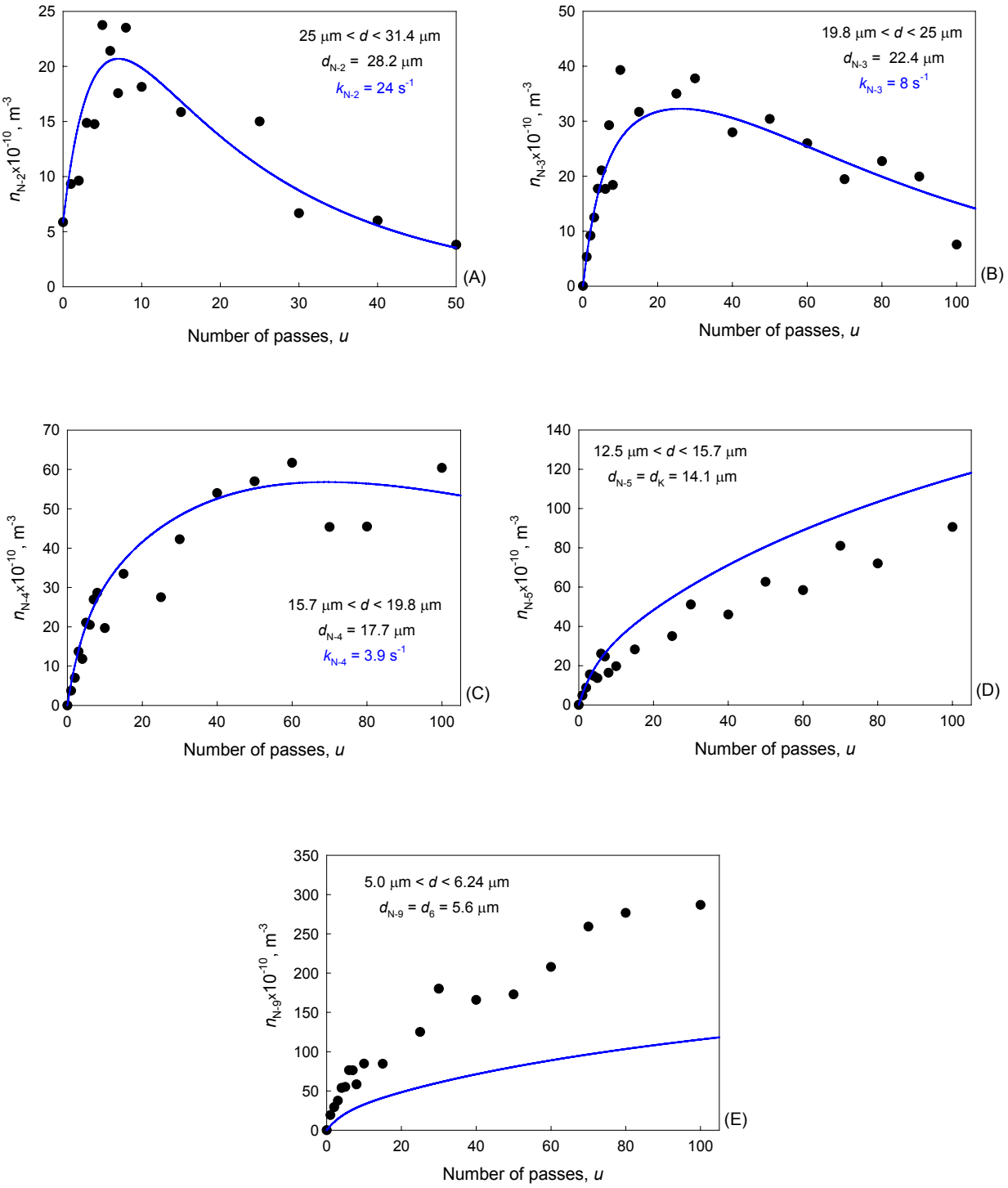

Figure 10. Number concentration of drops, as a function of the number of passes, along with the best fits constructed under the assumption for equal number probability for formation of smaller drops: (A) Third fraction of drops, d_{N-2}, with diameters between 25 and 31.4 μm; (B) Drops with diameters, d_{N-3}, between 19.8 and 25 μm; (C) Drops with diameters, d_{N-4}, between 15.7 and 19.8 μm; (D) Kolmogorov's drops with diameter, d_K, (E) Drops with diameter below the Kolmogorov's size. The experiments are performed with silicone oil-in-water emulsion, stabilized by 1 wt % Brij 58 (+150 mM NaCl) at $\Phi = 0.01$.

5.2.C. Non-equal probability for formation of smaller drops. As a next step in the data interpretation, we try to determine the value of $p_{S,q}$ under the assumption that the values of $p_{S,S-q}$ are the same for arbitrary s. In other words we suppose that $p_{S,S-q}$ does not depend on the diameter of the breaking drops. This assumption corresponds to so-called "self-similarity" mode of drop breakage [12-13].

The value of $p_{N,N-1}$ for all studied systems cannot be determined with sufficient accuracy from the experimental data for $n_{N-1}(u)$, because no increase of the concentration n_{N-1} with u is observed experimentally, due to the low initial concentration of the largest drops in the premix, $n_N^0 / n_{N-1}^0 \sim 0.1$, see Figure 8A. On the other hand, the ratio $n_{N-1}^0 / n_{N-2}^0 \sim 3$, which means that the number concentration of drops with diameter d_{N-2}, generated from larger drops with diameter d_{N-1}, is comparable or higher than their initial concentration, n_{N-2}^0. Thus, the value of $p_{N-1,N-2}$ will affect significantly the experimental function $n_{N-2}(u)$. For that reason we fitted the experimentally determined dependence of n_{N-2} (u) by using as adjustable parameters $p_{N,N-1} = p_{N-1,N-2}$ and $p_{N,N-2}$, whereas the values of k_N, k_{N-1} and k_{N-2} were taken from the best fits, describing the evolution of a given fraction of drops, when the latter are the largest ones in the emulsion. For silicone oil-in-water emulsion, the values of k_N, k_{N-1} and k_{N-2} were 293 s^{-1}, 129 s^{-1} and 24 s^{-1}, respectively. In this way, we were able to determine $p_{N-1,N-2} = p_{N,N-1} = 0.45 \pm 0.05$. However, the value of $p_{N,N-2}$ cannot be obtained with sufficient accuracy, due to the low initial concentration of the largest drops.

If we use the value $p_{N,N-1} = 0.45 \pm 0.1$ and fit the entire set of data for $n_{N-1}(u)$, the value of k_{N-1} changes from 129 s^{-1} to 123 s^{-1}, which is in the frame of our accuracy. Thus we can conclude that $k_{N-1} = 125 \pm 20$ s^{-1} for the emulsion under consideration.

The value of k_{N-2} also slightly depends on the values of $p_{S,N-2}$. It varies between 20 and 30 s^{-1} when $p_{N-1,N-2}$ varies between 0.45 and 0.6 (this is the range of values giving acceptable fit to the experimental data for $n_{N-2}(u)$, see Figure 9C). Therefore, $k_{N-2} = 25 \pm 5$ s^{-1} was accepted for the further consideration. It should be noted that the values of k_{N-1}, k_{N-2} obtained from the best fits to the entire curves for n_{N-1} (u) and n_{N-2} (u), using $p_{N-1,N-2} = p_{N,N-1} = 0.45 \pm 0.05$, agree with those obtained from the last part of the curves, when the respective drops are the largest ones in the emulsion.

To fit the experimental curve for $n_{N-3}(u)$, we fixed the values $p_{N,N-1} = p_{N-1,N-2} = p_{N-2,N-3} = 0.45$, and used the values of k_N, k_{N-1} and k_{N-2} determined from the fits for the larger drops. Thus we have three adjustable parameters to fit the data for $n_{N-3}(u)$: $p_{N-1,N-3} = p_{N,N-2}$, $p_{N,N-3}$, and k_{N-3}. The value of $p_{N,N-3}$ affects very slightly the theoretical curve $n_{N-3}(u)$, so that this value cannot be determined accurately from the fit. Thus from the best fit we were able to determine the values $p_{N-1,N-3} = p_{N,N-2} = 0.325 \pm 0.025$ and $k_{N-3} = 8 \pm 1.5$ s^{-1}.

Following similar procedure, we were able to determine from the fits to the data for the smaller drops $k_{N-4} = 4 \pm 1$ s^{-1} and $k_{N-5} = 1.5 \pm 1 s^{-1}$. Note that the value of k_{N-5} is very close to zero, which is to be expected because the Kolmogorov size for this system is 13.6 μm,

which falls in the interval of the drops under consideration. For the probabilities of daughter drop formation we obtained $p_{S,S-3} = 0.094 \pm 0.002$ and $p_{S,S-4} \approx 0.02 \pm 0.01$.

In conclusion, the values of the breakage rate constants are determined with an accuracy of about 20 %. The values of $p_{S,q}$ decrease with the decrease of q, see Figure 11. It is seen that around 45 % of the volume of a breaking drop with diameter d_S is transformed into drops with diameter d_{S-1}, whereas 32 % is transformed into drops with size d_{S-2}. The remaining 23 % of the drop volume transform into even smaller drops. We have no sufficient accuracy to determine precisely the values of $p_{S,S-4}$ and the subsequent constants characterizing the generation of smaller drops.

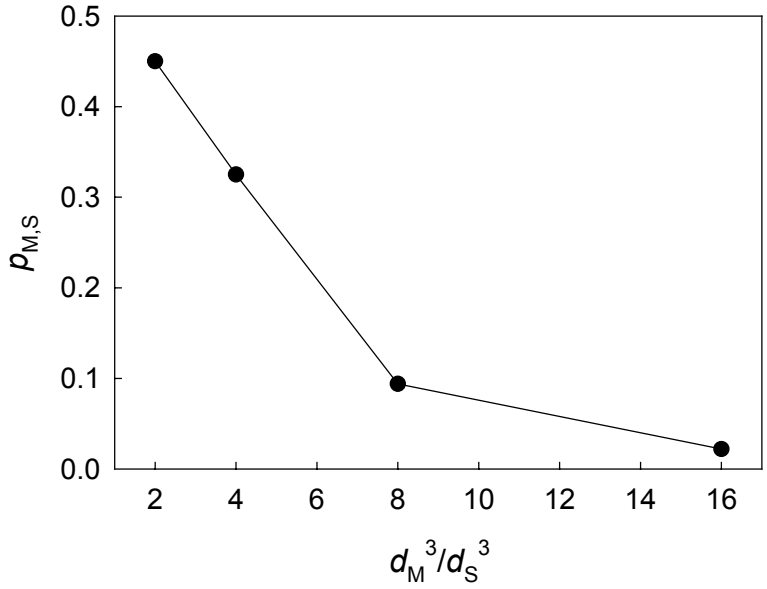

Figure 11. Average volume probability for formation of drops with size d_S after breaking a drop with diameter d_M, as a function of the volume ratio for the breaking and forming drops, d_M^3/d_S^3. The points are determined from the best fits to the experimental data for silicone oil-in-water emulsions, stabilized by 1 wt % Brij 58.

5.3. Breakage rate constant as a function of drop diameter.

In this subsection we present the dependence of k_S on d_S, as determined from the experimental data under the assumption for self-similarity of drop breakage ($p_{S,S-q}$ are considered independent of s). The procedure for determination of k_S is described in the previous subsection.

(A) Effect of the oil viscosity on k_{BR}. To check how the oil type and viscosity affect the dependence $k_{BR}(d)$ we performed experiments with oil-in-water emulsions stabilized by 1 wt % Brij 58 (+150 mM NaCl) by using as oil phase: silicone oil with viscosity 50 mPa.s; silicone oil with viscosity 96 mPa.s, or soybean oil with viscosity 50 mPa.s. The mean surface-volume diameter for all initial emulsions (premixes) was around 34 μm, see Table 1.

The emulsification conditions are described in section 3.1. The applied pressure is around 10^5 Pa, and the residence time is around 2 ms.

The dependencies $k_{BR}(d)$ for the studied oils are presented in Figure 12. For the emulsions prepared with silicone oil and SBO, both with η_D = 50 mPa.s, k_{BR} decreases from 120 down to 1 s^{-1} while decreasing the drop diameter from 35 to 15 μm. For these two oils, the values of k_{BR} are almost the same in the frame of our accuracy for d between 35 and 15 μm. For both systems, the breakage rate constant becomes virtually 0 when d reaches the Kolmogorov diameter, estimated by eq 2. On the other hand, the value of k_{BR} for drops with diameter 45 μm, for SBO-in-water emulsion, is larger than 500 s^{-1}, whereas the value for silicone drops with the same diameter is around 300 s^{-1}, which indicates that the interfacial tension is more important for the larger drops (the interfacial tension for SBO is smaller than that for silicone oil, 7.4 vs 10.9 mN/m). It seems that changes in the interfacial tension do not affect strongly k_{BR} for drops with diameter close to d_K.

On the other hand, when the viscosity of the oil phase increases from 50 to 100 mPa.s (cf. the red and pink points in Figure 12), the value of k_S decreases from 300 to 100 s^{-1} for drops with average diameter of 45 μm, and from 120 to 18 s^{-1} for drops with average diameter of 35 μm. Note that the interfacial tension for these two systems is the same (≈ 10.5 mN/m). Hence, the lower values of k_{BR} are due to the higher oil viscosity.

In conclusion, the oil viscosity significantly affects the breakage rate constant for systems, in which the density of energy dissipation and the interfacial tension are similar. The interfacial tension slightly affects k_{BR} for oils with similar viscosity (for drops which are not much larger than d_K).

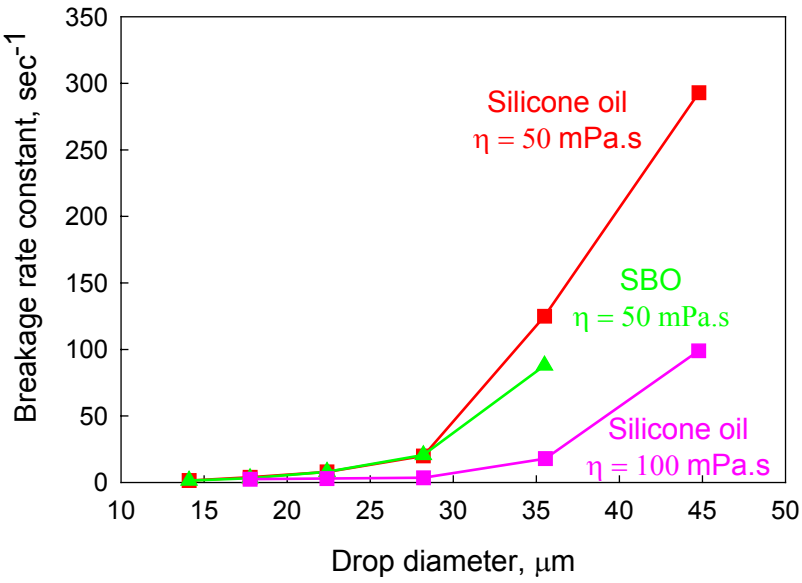

Figure 12. Breakage rate constants, as functions of drop diameter, for emulsions stabilized by 1 wt % Brij 58 (+150 mM NaCl) for silicone oil with η_D = 50 mPa.s (red squares); silicone oil with η_D = 100 mPa.s (pink squares); and soybean oil with η_D = 50 mPa.s (green triangles). The emulsification conditions are presented in Table 1.

(B) Effect of average power density on the dependence of k_{BR} on d

The effect of hydrodynamic conditions on k_{BR} was studied with SBO-in-water emulsions. The mean drop diameter in the initial emulsions (premixes) was the same, but the emulsification experiments were performed at two different driving pressures, 1 and 2 atm, in the narrow-gap homogenizer. The obtained dependencies $k_{BR}(d)$ are shown in Figure 13A. The results show that k_{BR} increases more than 40 times when ε is increased from 0.49×10^5 to 1.92×10^5 J/kg.s, see Table 1. The plot of the dependence k_{BR} vs. d/d_K is presented in Figure 13B. It is seen from the figure that k_{BR} is around 2 times higher for emulsions prepared at higher pressure, for drops with diameter two times larger than d_K.

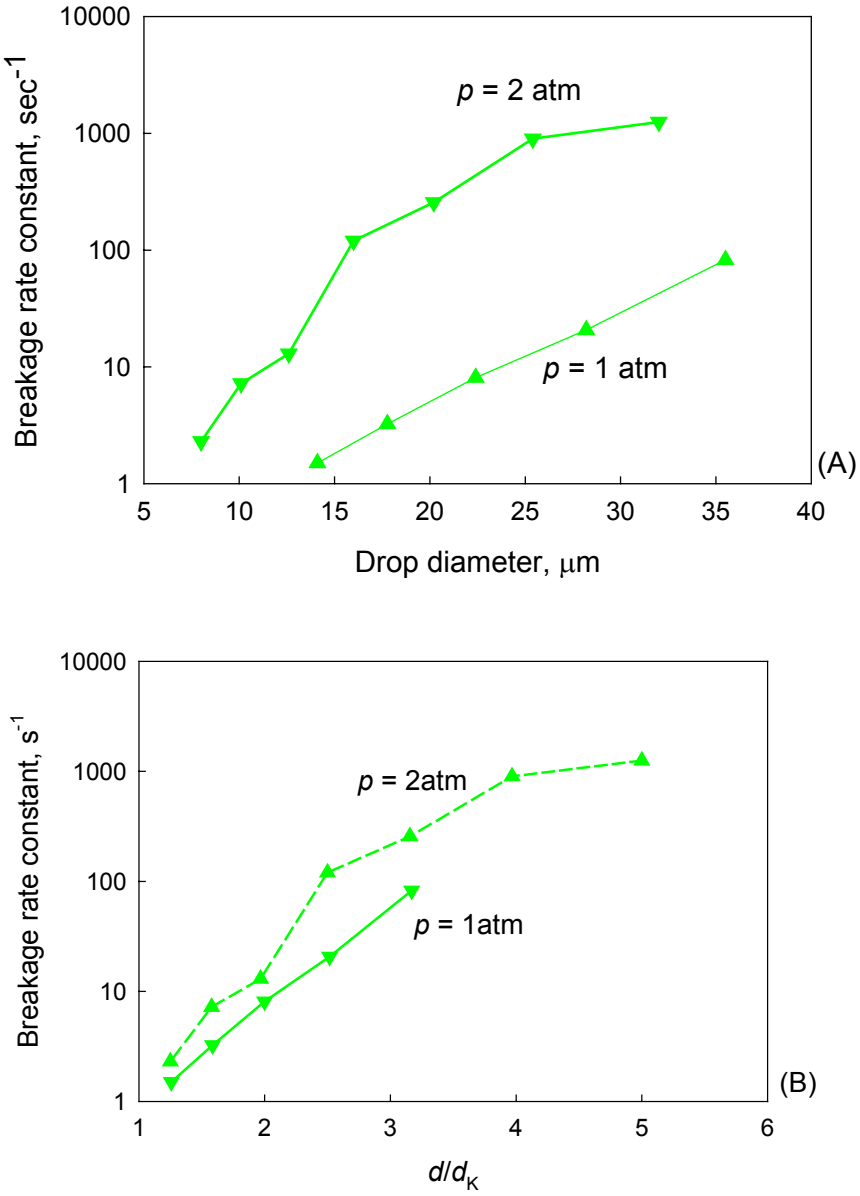

Figure 13. Breakage rate constants as a function of: (A) Drop diameter; and (B) Normalized drop diameter, d/d_K, for soybean oil-in-water emulsions stabilized by 1 wt % Brij 58 (+150 mM NaCl) at two different driving pressures, see also Table 1.

6. Theoretical models for the dependence of the breakage rate constant on drop diameter and their comparison with the experimental results.

Models containing explicit expressions for k_{BR} are proposed in Refs. 1-4,25. In this section we briefly describe these models (and some modifications), and compare them with our experimental results.

6.1. Model proposed by Tavlarides and Coulaglou [1].

The model for the rate of drop breakage, proposed by Coulaglou and Tavlaridies [1], is based on the assumption that k_{BR} is a product of the fraction of drops (from the total number of drops in the emulsion) having energy sufficiently large to induce drop breaking and of the reciprocal time required for drop breakage to occur:

$$k_{BR} = \left(\frac{1}{breakage\ time}\right)\left(\begin{matrix}fraction\ of\\drops\ breaking\end{matrix}\right) = \frac{1}{\tau_{BREAKAGE}}\exp\left(-\frac{E_\sigma}{\bar{E}}\right) \tag{18}$$

Here the exponential factor is assumed to be the ratio of the surface energy required for drop deformation and the mean kinetic energy of the turbulent eddies. The drop surface energy is estimated as:

$$E_\sigma \sim \pi d^2 \sigma_{OW} \tag{19}$$

The mean turbulent kinetic energy of the eddies with size equal to the drop size, d, can be found from the theory of turbulence [1]:

$$\bar{E} \sim \pi \rho_D d^3 \overline{u^2} \big/ 6 \tag{20}$$

where ρ_D is the mass density of the dispersed phase and $\overline{u^2}$ is the mean square velocity of the eddies. For the inertial subrange, $\overline{u^2}$ is given by

$$\overline{u^2} \sim \varepsilon^{2/3} d^{2/3} \tag{21}$$

The breakage time entering eq 18 is assumed to be equal to the so-called “deformation time”, needed for deforming the drop to a sufficiently large aspect ratio, so that Rayleigh type of capillary instability could occur. The respective equation for the deformation time depends on the Reynolds number in the drops, defined as [27]:

$$\mathrm{Re}_{DR} = \frac{U_{DR} d \rho_D}{\eta_D} \tag{22}$$

where U_{DR} is the velocity of the liquid inside the drops, and η_D is the dynamic viscosity of the dispersed phase. If $\mathrm{Re}_{DR} > 1$ (drops with viscosity similar or smaller than that of the surrounding fluid), the deformation time is estimated by comparing the force acting on the drops, due to fluctuations in the dynamic turbulent pressure, and the acceleration of the drop subdomains , $\frac{\nabla p}{\rho_C} \sim \frac{\partial \mathrm{v}}{\partial t}$ (see section 127 in Ref. [27]). The respective expression for the deformation time reads (cf. with eq 127.6 in Ref. [27]):

$$\tau_{DEF} = \frac{d^{2/3}}{\varepsilon^{1/3}} \sqrt{\frac{\rho_D}{\rho_C}} \qquad \mathrm{Re}_{DR} > 1 \tag{23}$$

Combining eqs 18-21, one derives the following equation for the rate constant of drop breakage at $\mathrm{Re}_{DR} > 1$ [1]:

$$k_{BR}(d) = a_1 \frac{\varepsilon^{1/3}}{d^{2/3}} \sqrt{\frac{\rho_C}{\rho_D}} \exp\left(-a_2 \frac{6\sigma_{OW}}{\rho_D \varepsilon^{2/3} d^{5/3}} \right) \qquad \mathrm{Re}_{DR} > 1 \tag{24}$$

where a_1 and a_2 are unknown constants of the order of unity.

On the other hand, if $\mathrm{Re}_{DR} < 1$, which is the case of viscous dispersed phase, the deformation time can be estimated by neglecting the acceleration term (quasi-stationary approximation) and comparing the pressure fluctuations with the viscous stress in the drops. The respective equation reads (cf. with eq 127.7 in Ref. [27]):

$$\tau_{DEF} = \frac{\eta_D}{\varepsilon^{2/3} d^{2/3} \rho_C} \; ; \qquad \mathrm{Re}_{DR} < 1 \tag{25}$$

Note that in this case, the deformation time increases with the viscosity of the dispersed phase, η_D, whereas the deformation time does not depend on drop viscosity in eq 23. Furthermore, eq 25 predicts that the deformation time decreases with drop diameter for viscous drops, whereas eq 23 (for non-viscous drops) predicts the opposite trend.

Combining eqs 18-20 and 25, we obtain the following expression for the breakage constant of drops with viscous disperse phase ($\mathrm{Re}_{DR} < 1$):

$$k_{BR}(d) = \frac{\rho_C d^{2/3} \varepsilon^{2/3}}{\eta_D} \exp\left(-\frac{6\sigma_{OW}}{\rho_D \varepsilon^{2/3} d^{5/3}} \right) \; ; \qquad \mathrm{Re}_{DR} < 1 \tag{26}$$

One sees from eq 24 that the main parameters, governing the rate of breakage for $Re_{DR} > 1$, are the average power density, ε, which characterises the hydrodynamic conditions during emulsification, and the interfacial tension, σ_{OW}, which depends on the used surfactant. For $Re_{DR} < 1$, the viscosity of the oil phase, η_D, also affects the rate of drop breakage, see eq 26.

6.2. Comparison of the experimental data with the model by Coulaglou and Tavlarides [1]

We calculated the value of the Reynolds number in the drops by eq 22, and found that $Re_{DR} < 1$ for the drops with $d < 40$ μm, for all studied emulsions prepared at $p = 1$ atm. For SBO-in-water emulsions, prepared at $p = 2$ atm, $Re_{DR} \approx 1$ for drops with diameter 30 μm. This means that the value of Re_{DR} is lower or close to 1, and we should use eq 26, to fit the experimental data for all emulsions, in the frame of the model from ref 1.

To compare the experimental data and the theoretical dependence, we constructed the plot $\ln[k_{BR} \times \eta_D/(\rho_C\, d^{2/3}\, \varepsilon^{2/3})]$ versus $(d_K/d)^{5/3}$, which should correspond to a "master" straight line, according to eq 26; d_K is calculated by eq 2. As seen from Figure 14, the experimental points do not fall on a straight line or on a single "master" curve. One can conclude from this comparison that the model proposed by Coulaglou and Tavlaridies [1] does not describe adequately the experimental data for the dependence of k_{BR} on the drop diameter and on the viscosity of the oil phase.

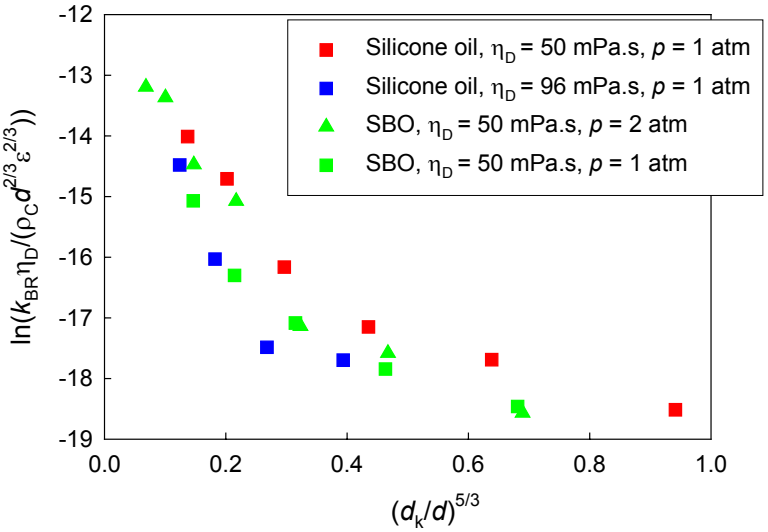

Figure 14. Dependence of the logarithm of the normalized breakage rate constant, $\frac{k_{BR}\eta_D}{\rho_C d^{2/3}\varepsilon^{2/3}}$, as a function of $(d_K/d)^{5/3}$ for the various systems (see eq 26).

6.4. Model proposed by Prince and Blanch [4]

In this model the breakage rate constant is assumed to be proportional to the frequency of drop-eddy collisions, multiplied by the collision efficiency [4]:

$$k_{BR} = \left(eddy - drop\ \ collision\ \ frequency\right)\left(breakage\ efficiency\right) \tag{27}$$

The probability for drop-eddy collision is estimated under the assumption that the drops and eddies can be considered as molecules in the kinetic theory of gases. Thus the collision frequency $h(d)$ between drops of size d and eddies of a size that can break these drops (i.e., eddies with size equal or smaller than drop diameter) is presented as [4]:

$$h\left(d\right) = \int_{n_e} S_{eq}\left(u_e^2 + u_d^2\right)^{1/2} n_d dn_e \tag{28}$$

where $S_{eq} = \frac{\pi}{4}\left(d_e + d\right)^2$ is the collision cross-section area; d_e is eddy size; d is drop diameter; n_d is number concentration of drops with size d; dn_e is the number concentration of eddies with size between d_e and $d_e+\delta d_e$; u_e is the mean velocity of eddies with size d_e; and u_d is the mean drop velocity.

To apply eq 28, one needs to know the number concentration of eddies with given size, d_e. This concentration can be determined from the expression, derived by Azbel and Athanasios [4, 28]:

$$\frac{dN\left(k\right)}{dk} = \frac{0.1k^2}{\rho_C} \tag{29}$$

where $N(k)$ is the number of eddies of wave number k per unit mass of the fluid, and ρ_C is the mass density of the continuos phase.

The efficiency of drop breakage is experseed by the following equation:

$$E\left(d\right) = \exp\left(-\frac{E_\sigma}{E_{KIN}}\right) \tag{30}$$

where E_σ is the drop surface energy given by eq 19, whereas E_{KIN} is the kinetic energy of the eddy, expressed as:

$$E_{KIN} = 0.43\rho_C\pi(2/k)^{11/3}\varepsilon^{2/3} \tag{31}$$

Thus, the equation for the breakage rate constant, in this model [4], reads:

$$k_{BR}(d) = 0.1\frac{\pi}{4}\varepsilon^{1/3}\int_{2/d}^{2/\lambda_0}\left(\frac{2}{k}+d\right)^2\left(8.2k^{-2/3}+1.07d^{2/3}\right)^{1/2}k^2\exp\left(-\frac{E_\sigma}{E_{KIN}}\right)dk \tag{32}$$

where λ_0 is the size of the smallest eddies in the system.

If we assume that most efficient for drop breakage are the drop collisions with eddies of size equal to that of the drops (because these eddies have largest kinetic energy [27,29]), one derives the following simple expression for the rate constant of drop breakage:

$$k_{BR}(d) \sim \frac{\varepsilon^{1/3}}{d^{2/3}}\exp\left(-\frac{\sigma_{OW}}{\rho_C d^{5/3}\varepsilon^{2/3}}\right) \tag{33}$$

The pre-exponential term in the above equation arises from the frequency of eddy-drop collisions, whereas the exponential term accounts for the breakage efficiency. It is seen that this equation is similar in structure to eq 24, but the density of the continuous phase, instead of that of the dispersed phase, appears in the exponential term (see the discussion on this point in ref 4). It is obvious from eq 33 that we cannot decribe the experimentally observed dependence of k_{BR} on the oil viscosity by this model, because this viscosity does not appear in the equation.

Following the idea of Callabrese et al. [8-10], we can include the dissipated energy inside the drops in the collision efficiency to account for the contribution of the oil viscosity:

$$E_{DIS} = \frac{\pi}{6}d^3\tau_D = \frac{\pi}{6}d^3\left(\eta_D\frac{\sqrt{\frac{\rho_C}{\rho_D}}\varepsilon^{1/3}d^{1/3}}{d}\right) \tag{34}$$

where τ_D is the viscous stress inside the drop. Hence, the "activation" energy, which opposes drop deformation, is presented as a sum of E_{DIS}, eq 34, and the surface enrergy, E_σ, eq 19. The respective equation for the breakage rate constant reads:

$$k_{BR}(d) \sim A_0\frac{\varepsilon^{1/3}}{d^{2/3}}\exp\left(-A_1\frac{9.3\left(\sigma_{OW}+0.136\sqrt{\frac{\rho_C}{\rho_D}}\varepsilon^{1/3}d^{1/3}\eta_D\right)}{\rho_C\varepsilon^{2/3}d^{5/3}}\right) \tag{35}$$

where the unknown parameters A_0 and A_1 are included, because the expressions used to construct eq 35 are approximate estimates. The constants A_0 and A_1 can be determined from the best fits to available experimental data.

6.5. Comparison of the experimental data for k_{BR} with the predictions of eq 35.

According to eq 35, the experimental data for the various systems should fall on a master line, if the following scaling is applied:

$$\ln\left(\frac{k_{BR}(d)d^{2/3}}{\varepsilon^{1/3}}\right) \sim -A_1\left(\frac{d_K}{d}\right)^{5/3} - A_1A_2\eta_D\left(d_K^{8/3}\rho_C\rho_D\varepsilon^{2/3}\right)^{-1/2}\left(\frac{d_K}{d}\right)^{4/3} \sim A_1 f\left(\frac{d_K}{d},\eta_D,\rho_C,\rho_D,\varepsilon^{2/3}\right) \quad (36)$$

where d_K is defined by eq 2; A_0 and A_1 are adjustable constants and all remaining parameters are known from the experiment. As seen from Figure 15, the experimental data for all studied systems follow a linear dependence down to the drop size corresponding to the Kolmogorov's diameter (the last points on the right-hand side). Furthermore, the data for all systems fall on the same line, which indicates that eq 35 adequately represents the dependence of k_{BR} on oil viscosity and drop diameter (at least for the drops larger than Kolmogorov's diameter). The values of the adjustable constants A_0 and A_1, found from the best fits to the data, are presented in Table 5. For all systems A_0, which plays the role of the "steric factor" in the molecular collision theory of chemical kinetics, is of the order of 0.1, whereas the values of A_1 are very close to 1. These values of A_0 and A_1 are very reasonable from physical viewpoint and indicate that eq 35 describes correctly the process under consideration.

For drops having diameter close to the Kolmogorov size, the deviation of the experimental data from the straight line is well pronounced for all studied emulsions. This is most probably due to the lack of accuracy in the used procedure for determination of k_{BR} for these small drops. Note that for all systems, this is the 6th fraction of drops (starting from the largest ones) and their evolution is strongly affected by the values of $p_{S,m}$, which are not known with high precision.

Table 5. Numerical values of the constants A_0 and A_1, determined from the best fits to the experimental data, see Figure 16.

η_D, cP	σ_{OW}, mN/m	$\varepsilon\times10^5$, J/(kg.s)	A_0	A_1	r^2
50 (SBO)	7.4	0.49	0.08 ± 0.03	1.2 ± 0.2	0.992
50 (SBO)	7.4	1.92	0.1 ± 0.02	0.99 ± 0.09	0.9983
50 (silicone oil)	10.9	0.53	0.1 ± 0.01	1.0 ± 0.05	0.998
96 (silicone oil)	10.3	0.56	0.1 ± 0.05	1.1 ± 0.02	0.9795

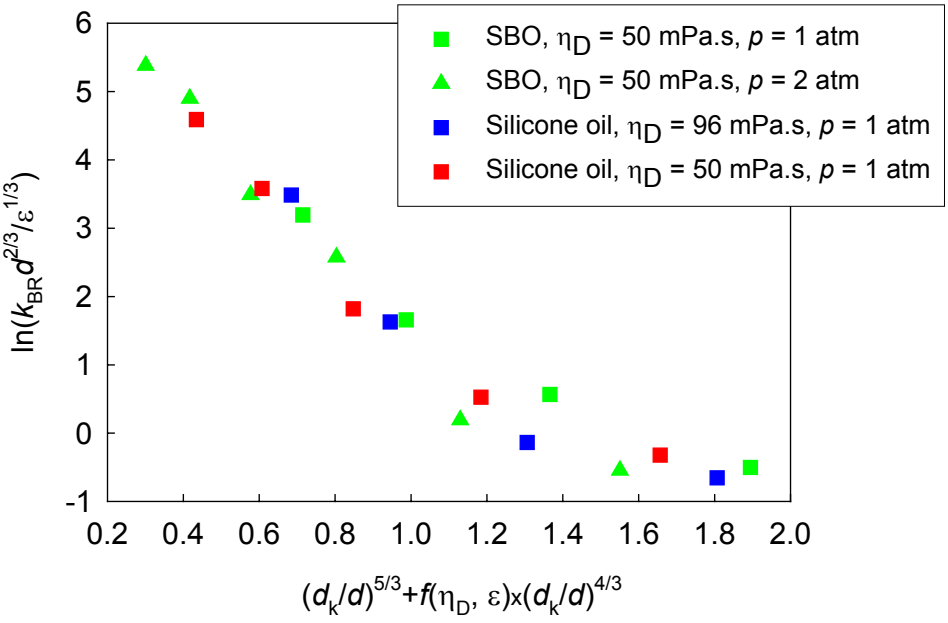

Figure 15. Dependence of the logarithm of the normalized breakage rate constant, $\frac{k_{BR}d^{2/3}}{\varepsilon^{1/3}}$, as a function of the normalized diameter, for the various systems (see eq 36).

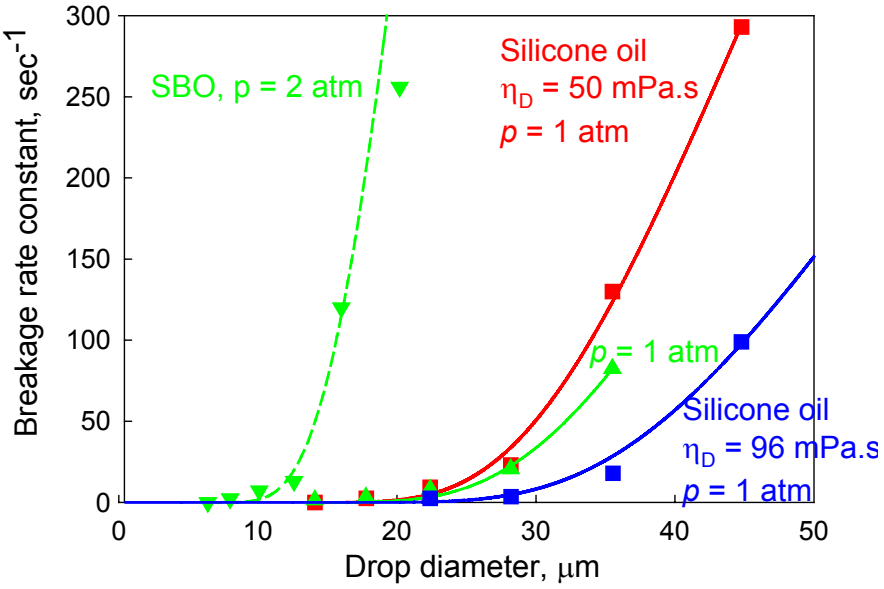

Figure 16. Breakage rate constant vs drop diameter for the various emulsions studied, along with the best fits by using eq 35 with A_0 and A_1 from Table 5.

7. Conclusions.

Systematic set of experiments is performed to monitor the evolution of the drop size distribution, as a function of emulsification time, in emulsions subject to turbulent flow in a narrow-gap homogenizer. The experimental data are interpreted by using a kinetic scheme, which allows us to determine the rate constant of drop breakage, as a function of drop diameter. The kinetic scheme is based on the assumption that the drop breakage process is an irreversible reaction of first order and that multiple drops of various sizes are formed in the breakage event. From the experimental data, the breakage rate constants in the studied emulsions are determined, as functions of the physical properties of the system – drop size, viscosity of the oil phase, and hydrodynamic conditions during emulsification. The results show that the breakage rate constants rapidly decrease with the decrease of drop diameter and become virtually zero, when the drop diameter reaches the Kolmogorov's size. At given drop size and oil viscosity, a four-fold increasing in the power dissipation rate leads to an increase of the breakage rate constant by more than 40 times. On the other hand, at similar hydrodynamic conditions, a 2-fold increase of the oil viscosity leads to more than a 3-fold decrease of the breakage rate constant.

The obtained experimental dependencies of k_{BR} on drop diameter are compared with theoretical models, proposed in the literature, and their modifications. It is shown that k_{BR} can be considered as a product of the collision frequency between the drops and eddies with similar size, multiplied by a factor accounting for breakage efficiency. A modified expression for the breakage efficiency is proposed, which includes the contributions of both the surface extension energy and the energy dissipation inside the drops, in the process of drop deformation by the turbulent stresses. The theoretical dependence is in a reasonably good agreement with the experimental data for all studied systems.

References:

1. Coulaloglou, C. A.; Tavlarides, L.L Description of interaction processes in agitated liquid-liquid dispersions. *Chemical Engineering Science* **1977**, *32*, 1289.
2. Tsouris, C.; Kirou, V. I.; Tavlarides, L.L. Drop size distribution and holdup profiles in a multistage extraction column. *AIChE Journal* **1994**, *40*, 407.
3. Tsouris, C.; Tavlarides, L.L. Breakage and coalescence models for drops in turbulent dispersions. *AIChE Journal* **1994**, *40*, 395.
4. Prince, M. J.; Blanch, H. W. Bubble coalescence and break-up in air-sparged bubble columns. *AIChE Journal* **1990**, *36*, 1485.
5. Razzaque, M. M; Afacan, A.; Liu, Sh.; Nandakumar, K.; Masliyah, J. H.; Sanders, R. S. Bubble size in coalescence dominant regime of turbulent air-water flow through horizontal pipes. *Inter. J. of Multiphase Flow* **2003**, *29*, 1451.
6. Kamp, A.M.; Chesters, A.K.; Colin, C.; Fabre, J. Bubble coalescence in turbulent flows: A mechanistic model for turbulence-induced coalescence applied to microgravity bubbly pipe flow. *Int. J. Multiphase Flow* **2001**, *27*, 1363.
7. Sprow, F.B. Distribution of drop sizes produced in turbulent liquid-liquid dispersion. *Chem. Eng. Sci.* **1967,** *22*, 435.
8. Calabrese, R.V.; Chang, T.P.K.; Dang, P.T. Drop breakup in turbulent stirred-tank contraction. Part I: Effect of dispersed-phase viscosity. *AIChE Journal* **1986**, *32*, 657.
9. Wang, C.Y.; Calabrese, R. V. Drop breakage in turbulent stirred-tank contractors. Part II: Relative influence of viscosity and interfacial tension. *AIChE Journal*, **1986**, *32*, 667.
10. Calabrese, R. V.; Wang, C.Y.; Bryner, N.P. Drop breakage in turbulent stirred-tank contractors. Part III: Correlations for mean size and drop size distribution. *AIChE Journal*, **1986**, *32*, 677.
11. Lagisetty, J. S.; Das, P. K.; Kumar, R.; Gandhi, K. S. Breakage of viscous and non-newtonian drops in stirred dispersions. *Chem. Eng. Sci.* **1986,** *41*, 65.
12. Narsimhan, G.; Ramkrishna, D.; Gupta, J. P. Analysis of drop size distribution in lean liquid-liquid dispersions. *AIChE Journal* **1980**, *26*, 991.
13. Narsimhan, G.; Nejfelt, G.; Ramkrishna, D. Breakage functions for droplets in agitated liquid-liquid dispersions. *AIChE Journal* **1984**, *30*, 457.
14. Kolmogoroff, A. N. Drop breakage in turbulent flow. *Compt. Rend. Acad. Sci. URSS,* **1949**, *66*, 825.
15. Hinze, J. O. Fundamentals of the hydrodynamic mechanism of splitting up in dispersion processes. *AIChE Journal* **1955**, *1*, 289.
16. Narsimhan, G. Model for drop coalescence in a locally isotropic turbulent flow. *J. Colloid Interface Sci*. **2004,** *272*, 197.

17. Kandori, K. Applications of microporous glass membranes: membrane emulsification; In: *Food Processing: Recent Developments*, A. G. Gaonkar, Ed.; Elsveier, Amsterdam, **1995**, pp. 113-142.

18. Kandori, K.; Kishi, K.; Ishikawa, T. Preparation of uniform silica hydrogel particles by SPG filter emulsification method. *Colloids Surf.* **1991**, *62*, 269-279.

19. Yoshizawa, H.; Ohta, H.; Hatate, Y. Novel procedure for monodispersed polymeric microspheres with high electrifying additive content by particle-shrinking method via SPG emulsification. *J. Chem. Eng. Japan* **1996**, *29*, 1027-1029.

20. Christov, N.; Ganchev, D. N.; Vassileva, N. D.; Denkov, N. D.; Danov, K. D.; Kralchevsky, P. A. Capillary mechanisms in membrane emulsification: oil-in-water emulsions stabilized by Tween 20 and milk proteins. *Colloids Surf. A* **2002**, *209*, 83.

21. Nakashima, T.; Shimizu, M. Advanced inorganic separative membranes and their developments. *Chem. Eng. Symp. Ser.* **1988**, *21*, 93-99.

22. Tcholakova, S.; Denkov, N. D.; Danner, T. Role of surfactant type and concentration for the mean drop size during emulsification in turbulent flow. *Langmuir* **2004**, *20*, 7444-7458.

23. Tcholakova, S.; Denkov, N. D.; Sidzhakova, D.; Ivanov, I. B.; Campbell, B. Interrelation between drop size and protein adsorption at various emulsification conditions. *Langmuir* **2003**, *19*, 5640-5649.

24. Hill, C. An introduction of chemical engineering kinetics & reactor design. John Wiley & Sons: New York, 1977, Chapter 8.

25. Narsimhan, J.; Gupta, J.P.; Ramkrishna, D. A model for transitional breakage probability of droplets in agitated lean liquid-liquid dispersions. *Chem. Eng. Sci.* **1979,** *34*, 257.

26. Orr, C. Emulsion droplet size data. In *Encyclopedia of Emulsion Technology*; Marcel Dekker: New York, 1983, Chapter 6.

27. Levich, V. G. Physicochemical Hydrodynamics, Prentice Hall, Englewood Cliffs, New Jersey, 1962.

28. Azbel, D.; Athanasios, I. L. A mechanism of liquid entrainment. In *Handbook of Fluids in Motion;* Cheremisinoff, N.; Ed.; Ann Arbor Science Publisher, Ann Arbor, MI, **1983,** p. 473.

29. Shreekumar, B.; Kumar, R.; Gandhi, K.S. Breakage of a drop of inviscid fluid due to a pressure fluctuation at its surface. *J. Fluid Mech*. **1996**, *328*, 1.